

GREENSTEIN, TYLER JOSEPH, M.S. Formation of Standards for Biosynthetic Studies of Bacillaene and Difficidin and Synthesis of Novel Enantioenriched Heterocycle via Desymmetrization. (2021)

Directed by Kimberly Petersen. 51 pp.

Polyketide synthases are multidomain enzymes that act as chemical assembly lines. Polyketides produced by polyketide synthases play a vital role within bacteria, such as providing it the necessary protection to defend against other bacteria. Two polyketides of interest have been bacillaene and difficidin, which reside from *Bacillus* species. Structurally, they contain  $\beta$ -branching that is atypical for polyketides. Since the enzymes and gene clusters of these polyketides are known, sequencing and production of the enzymes responsible for these  $\beta$ -branching patterns is possible. Previous work of the Reddick group accomplished this by reacting an acetoacetyl group with *pksI* and *dfnM* separately, which are the enzymes responsible for producing the  $\beta$ -branching for bacillaene and difficidin, respectively, and analyzed the products via mass spectrometry. With this data, there was confirmation that the mass corresponding to the desired  $\beta$ -branching was present; however, it was difficult to verify that the enzymes produced only their respective  $\beta$ -branching, as the  $\beta$ -branching of these polyketides are isomers. In the first sections of this work, the formation of standards for these  $\beta$ -branching mimics is accomplished by performing a coupling reaction between a carboxylic acid and a thiol. The mimics and the standards, which are chemically similar, will then be given to a member of the Reddick group to be subjected to gas chromatography mass spectrometry to obtain their fragmentation patterns, which will discern the  $\beta$ -branching pattern for these mimics. This will provide insight into the mode of action for these enzymes and, subsequently, the polyketide synthases.

Isomerism, much like polyketides, plays a vital role within biological systems. The difference between enantiomers can mean life or death, especially in terms of drug design and natural products. Some interesting and potentially harmful natural products come from those that contain the indole moiety. Being able to synthetically produce these natural products, especially enantioselectively, could prove to be both beneficial and difficult. Enantioselective catalysis can be a valuable tool for the creation of single enantiomers. Desymmetrization is a single step reaction where a prochiral molecule loses one or more symmetric features and is a technique for synthesizing enantiomers. Previous work of the Petersen group utilized desymmetrization reactions of malonic ester derivatives in the presence of a chiral Brønsted acid catalyst to achieve enantioenriched heterocycles. In the subsequent sections of this work, the malonic ester derivative containing an indole moiety is synthesized via a Knoevenagel Condensation reaction followed by a hydrogenation reaction. A desymmetrization is attempted utilizing this malonic ester derivative in the presence of a Brønsted acid catalyst to achieve a chiral heterocycle via a novel carbon-carbon bond formation. Once this is achieved, the desymmetrization reaction of the indole-containing starting material will be catalyzed by a chiral Brønsted acid catalyst to achieve an enantioenriched product.

FORMATION OF STANDARDS FOR BIOSYNTHETIC STUDIES OF BACILLAENE  
AND DIFFICIDIN AND SYNTHESIS OF NOVEL ENANTIOENRICHED  
HETEROCYCLE VIA DESYMMETRIZATION

by

Tyler Joseph Greenstein

A Thesis Submitted to  
The Faculty of The Graduate School at  
The University of North Carolina at Greensboro  
in Partial Fulfillment  
of the Requirements for the Degree  
Master of Science

Greensboro  
2021

Approved by

---

Committee Chair

APPROVAL PAGE

This thesis written by Tyler Joseph Greenstein has been approved by the following committee of the Faculty of The Graduate School at The University of North Carolina at Greensboro.

Committee Chair \_\_\_\_\_

Committee Member \_\_\_\_\_

\_\_\_\_\_

July 21<sup>st</sup>, 2021  
Date of Acceptance by Committee

July 19<sup>th</sup>, 2021  
Date of Final Oral Examination

## TABLE OF CONTENTS

	Page
LIST OF FIGURES .....	iv
CHAPTER	
I. POLYKETIDE INTRODUCTION MATERIAL .....	1
I.1 Polyketide Synthases .....	1
I.2 Bacillaene and Difficidin .....	5
I.3 Previous Work of the Reddick Group .....	7
II. SYNTHESIS OF POLYKETIDE STANDARDS .....	10
II.1 Present Works .....	10
II.2 Future Works and Conclusions .....	15
III. HETEROCYCLE FORMATION INTRODUCTION MATERIAL .....	17
III.1 Isomerism and Chirality .....	17
III.2 Indole-Containing Compounds .....	20
III.3 Asymmetric Synthesis .....	23
III.4 Brønsted Acid Catalysts .....	25
III.5 Previous Work of Petersen Group .....	27
IV. SYNTHESIS OF ENANTIOENRICHED HETEROCYCLE THROUGH CARBON-CARBON BOND FORMATION .....	31
IV.1 Present Works .....	31
IV.2 Future Works and Conclusions .....	34
V. EXPERIMENTAL PROCEDURES AND RESULTS .....	37
V.1 EDC Coupling of <b>1</b> and Benzyl Mercaptan .....	37
V.2 EDC Coupling of <b>1</b> and SNAC .....	38
V.3 Carboxylation of 2-Methylallylmagnesium Chloride .....	39
V.4 EDC Coupling of <b>5</b> and SNAC .....	40
V.5 Knoevenagel Condensation of Dimethyl Malonate and Indol-4- carboxyaldehyde .....	41
V.6 Hydrogenation of <b>7</b> .....	42
REFERENCES .....	43
APPENDIX A. NMR SPECTRA .....	46

## LIST OF FIGURES

	Page
Figure 1. Phosphopantetheinyl Arm .....	2
Figure 2. Formation of Model Polyketide .....	2
Figure 3. Formation of Alkene in Polyketide .....	3
Figure 4. Common Monomers Selected for Iterative or Modular AT PKSs .....	4
Figure 5. Bacillaene and Dihydrobacillaene .....	5
Figure 6. Difficidin and Oxydifficidin .....	7
Figure 7. Synthesis of $\beta$ -Branch in Bacillaene and Difficidin .....	8
Figure 8. Work Accomplished by Brittany Kiel .....	9
Figure 9. Simplified Reaction of Compound <b>3</b> and Compound <b>6</b> .....	10
Figure 10. Proposed Mechanism for EDC Coupling Reaction .....	11
Figure 11. Test Reaction Between Compound <b>1</b> and Benzyl Mercaptan .....	12
Figure 12. EDC Coupling Reaction Between Compound <b>1</b> and SNAC .....	12
Figure 13. Proposed Mechanism for Carboxylation of Compound <b>4</b> .....	13
Figure 14. Carboxylation of Compound <b>4</b> with Ammonium Chloride and Sodium Hydroxide Workup .....	13
Figure 15. Carboxylation of Compound <b>4</b> with Hydrochloric Acid and Sodium Hydroxide Workup .....	14
Figure 16. Isomerization of Compound <b>5</b> to Compound <b>1</b> .....	14
Figure 17. EDC Coupling Reaction Between Compound <b>5</b> and SNAC .....	15
Figure 18. Flowchart of Isomerism .....	17
Figure 19. Cyclohexane and 2-Hexene .....	18
Figure 20. The Enantiomers of Carvone .....	18
Figure 21. n-Butane and Newman Projections of n-Butane .....	19

Figure 22. L-Valine and D-Valine .....	20
Figure 23. ( <i>R, R</i> )-2-Bromo-3-Chloro-Butane and ( <i>S, R</i> )-2-Bromo-3-Chloro-Butane .....	20
Figure 24. Indole with Carbons Labelled .....	21
Figure 25. Resonance Structure of Indole and Alkylation at N-1 and C-3 of Indole .....	21
Figure 26. L-Tryptophan and Lysergic Acid Diethylamide (LSD) .....	22
Figure 27. Enantioselective Catalysis Example .....	24
Figure 28. Formation of Chiral Lactones Via Desymmetrization of Malonic Ester Derivatives by Chiral Brønsted Acid .....	24
Figure 29. Proposed Mechanism for Achiral Brønsted Acid on Malonic Ester Derivative .....	25
Figure 30. <i>p</i> -Toluenesulfonic Acid, Methanesulfonic Acid, and ( <i>R</i> )-TRIP Catalyst .....	26
Figure 31. Proposed Activation Complex Between Malonic Ester and ( <i>R</i> )-TRIP Catalyst .....	27
Figure 32. Work Accomplished by Jennifer Wilent .....	28
Figure 33. Work Accomplished by Amber Kelley .....	29
Figure 34. Pinner Reaction of Generic Nitrile and Alcohol .....	29
Figure 35. Proposed Synthetic Pathway to Form Compound <b>9</b> .....	32
Figure 36. Proposed Mechanism of Knoevenagel Condensation Between Generic Malonate and Aldehyde in the Presence of Piperidine .....	33
Figure 37. Knoevenagel Condensation Between Dimethyl Malonate and Indol-4- Carboxyaldehyde .....	34
Figure 38. Hydrogenation of Compound <b>7</b> .....	34
Figure 39. Desymmetrization of Compound <b>8</b> in the Presence of a Brønsted Acid .....	35
Figure 40. Attempt of Desymmetrization of Compound <b>8</b> in the Presence of <i>p</i> - Toluenesulfonic Acid .....	35
Figure 41. Decarboxylation of Compound <b>9</b> .....	36

# CHAPTER I

## POLYKETIDE INTRODUCTION MATERIAL

### I.1 Polyketide Synthases

Polyketide synthases (PKSs) are massive, multidomain proteins which have the potential to produce a wide variety of polyketides, each having their own unique purpose within an organism.<sup>1</sup> PKSs all fall under one of three major types which consist of Type 1, Type 2, or Type 3 PKSs. Type 1 is the most abundant type of polyketide synthases and differs from Type 2 and Type 3 by consisting of multifunctional enzymes organized into modules. These modules contain different domains, whose purpose is to either elongate the polyketide or functionalize it.

To initialize the polyketide formation process, there must be monomers present within a cell. A couple of the common monomers include acetyl-Coenzyme A (acetyl-CoA) and malonyl-Coenzyme A (malonyl-CoA). The first monomer, or the starting unit, begins at the loading module which contains an acyltransferase (AT) domain and an acyl carrier protein (ACP) domain.<sup>1</sup> The AT domain selects this starting unit and then loads it onto the ACP.<sup>1</sup> This loading process is achieved by the formation of a thioester linkage to the phosphopantetheinyl arm (Figure 1).<sup>1</sup>

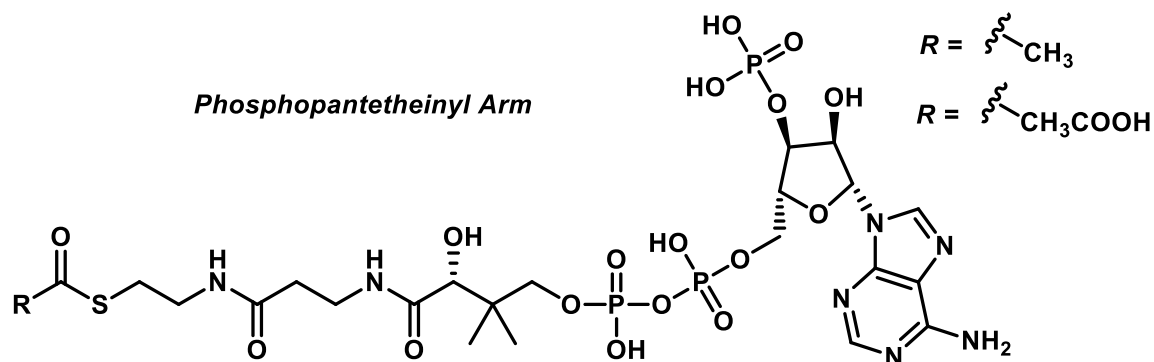


**Figure 1.** Phosphopantetheinyl Arm.

The ketosynthase (KS) of the first module after the loading module then obtains the growing chain of the polyketide and catalyzes the carbon-carbon bond formation, leaving the intermediate on the latest ACP domain.<sup>1</sup> Once the starting unit is loaded onto the PKS, the AT of the first domain selects another monomer and loads it onto the ACP of the first domain which is accomplished again by the phosphopantetheinyl arm.<sup>1</sup> The KS then catalyzes the formation of the carbon-carbon bond between starting unit and the new monomer, known as an extending unit, and again leaves it on the latest ACP (Figure 2).<sup>1</sup>

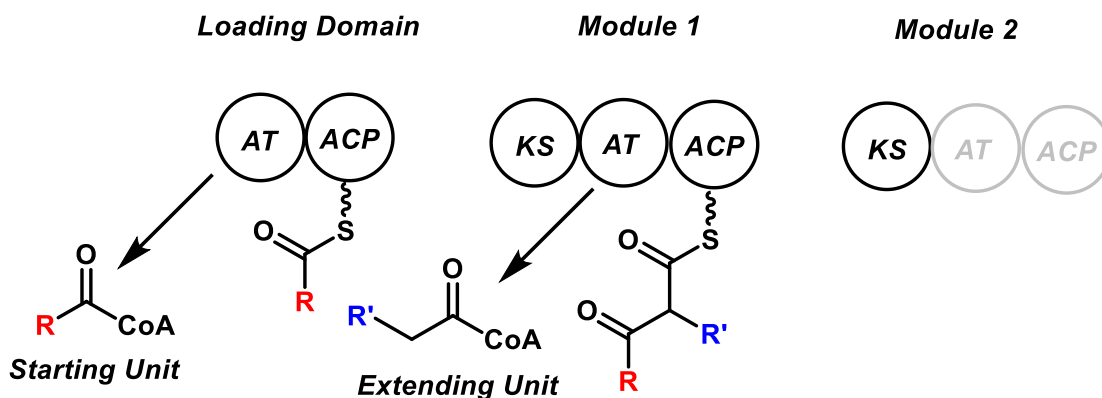


**Figure 2.** Formation of Model Polyketide. Red R groups come from the starting unit while blue R groups come from the extending unit.

This process then continues until the polyketide reaches the terminal domain where a thioesterase (TE) is present which catalyzes a macrolactonation to release the polyketide from the PKS.<sup>1</sup> Once the polyketide has been released, it can then go through further modification, such as cyclization or additional functionalization.

Between the AT domain and the ACP within each of the modules, there can be other processing domains which help to functionalize the polyketide. The four most common of these processing domains are as follows: dehydratase (DH) domain, methyltransferase (MT), ketoreductase (KR), and enoylreductase (ER). DH catalyzes dehydration reactions; MT attaches methyl groups at the  $\alpha$ -position of the polyketide intermediate; KR stereoselectively reduces the  $\beta$ -keto group and controls the  $\alpha$ -substituent; and ER stereoselectively reduces double bonds and controls the  $\alpha$ -substituent.<sup>1</sup> One interesting aspect of polyketide synthases is that to gain these different functionalities, each module must be comprised of a combination of these processing domains. For example, the formation of an alkene in a polyketide requires there to be both a DH and a KR present between the AT and ACP domains (Figure 3).

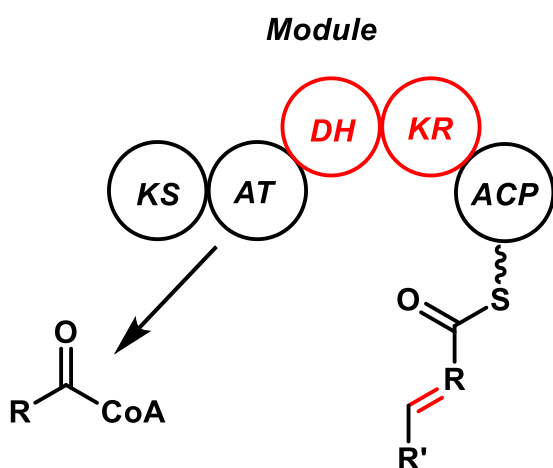


**Figure 3.** Formation of Alkene in Polyketide. *The red domains are responsible for the formation of the alkene.*

Type 1 PKSs specifically can be further characterized into either iterative or modular, as seen in Figure 4. Iterative Type 1 PKSs organize their domains in a cyclic fashion.<sup>2</sup> This allows the PKS to reuse the same domains on the same polyketide. Once the desired polyketide is obtained, the PKS releases it wherever necessary along this cyclic path. Modular Type 1 PKSs have its domains in a linear fashion where each domain is only used once, and the polyketide is removed at the end of this system.<sup>2</sup> Modular Type 1 PKSs can be separated further into either *cis*-AT or *trans*-AT PKSs. In the *cis*-AT system, the AT domain within each module is within the PKS whereas the *trans*-AT system has the AT domain outside of the PKS.<sup>2</sup> These *trans*-AT PKSs signal for the AT domains to work on the polyketide and then are released back into the cell once it has completed its work.<sup>2</sup>

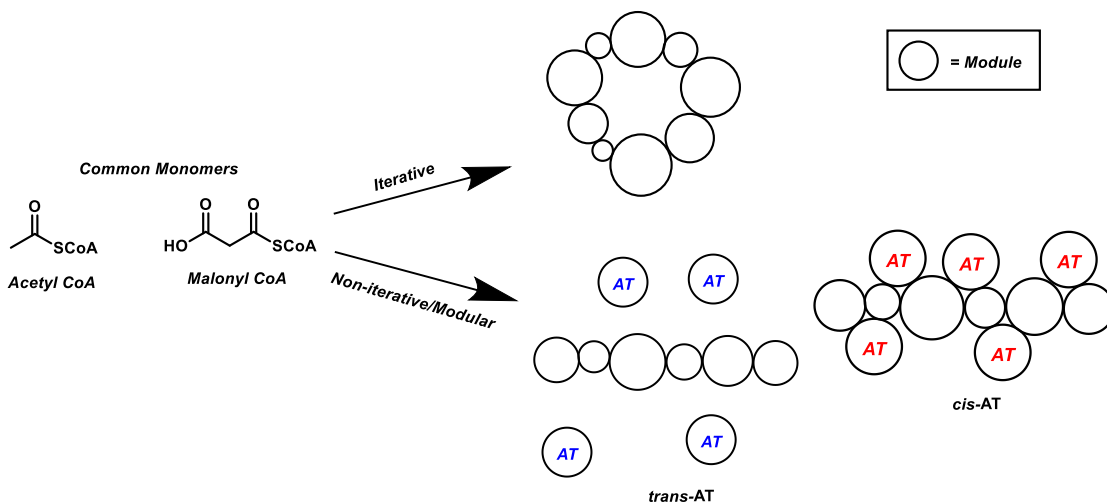


**Figure 4.** Common Monomers Selected for Iterative or Modular AT PKSs.

## 1.2 Bacillaene and Difficidin

The PKS gene cluster responsible for the formation of bacillaene (Figure 5), known as *pksX*, was partially sequenced in 1993.<sup>3</sup> The molecule was then first discovered in 1995 with its structure unknown.<sup>3</sup> The entirety of the genome was then sequenced in 1997, which revealed that the rest of the *pksX* gene cluster was not identified.<sup>3</sup> When the gene cluster was sequenced, it was determined to generate a *trans*-AT PKS in *Bacillus subtilis* 168.<sup>3</sup> The structure was finally identified, along with dihydrobacillaene (Figure 5), by scientists John Clardy and Frank Schroeder at Harvard in 2007 by extracts of *B. subtilis* strains.<sup>3</sup> The polyketide's main function comes in the form of an antibiotic which works to inhibit the synthesis of prokaryotic proteins, although its specific target remains unknown.

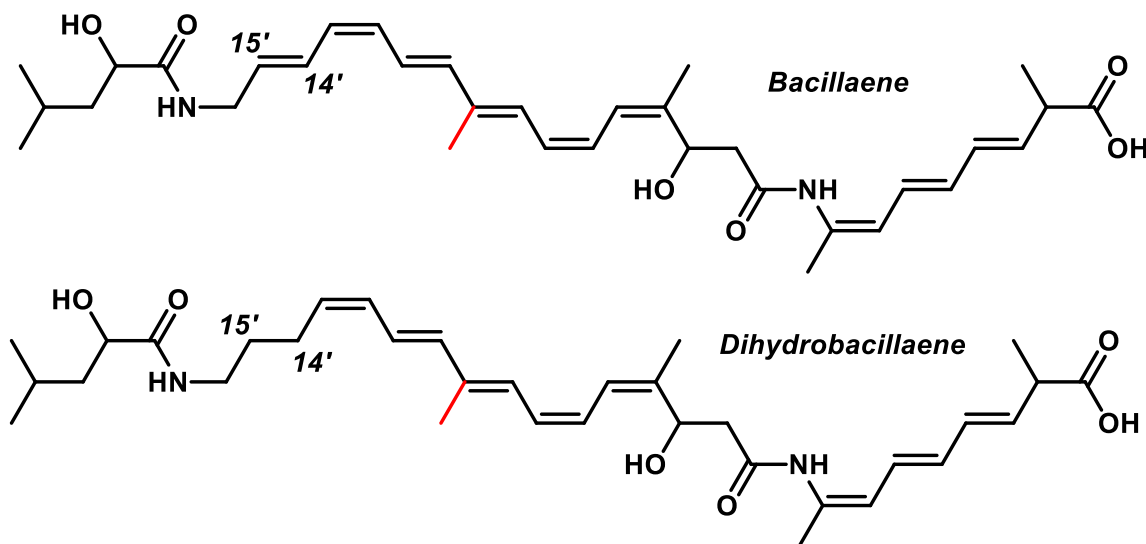


**Figure 5.** Bacillaene and Dihydrobacillaene. The red bond indicates the abnormal  $\beta$ -branching and the position of the difference between the two are marked.

The structures of bacillaene and dihydrobacillaene have been worked on for much of the late 1990s; however, this was difficult due to its structure being unstable with the

series of conjugated bonds within the molecule and its linear nature. One of the biggest revelations to the compounds structure came through the work of Kelleher, Walsh and coworkers who identified building blocks and intermediates attached to the *pksX* enzymes using Fourier-transform ion cyclotron resonance mass spectrometry (FT-ICR-MS).<sup>4</sup> Through this method, they were able to determine that the *trans*-AT preferably loaded malonyl-CoA. This also led to the discovery of a novel reaction sequence known as  $\beta$ -branching, which converts a  $\beta$ -keto function into a carbon branch, usually a methyl group.<sup>5</sup> Further work by Chen et. al. used genetic mutations of the *pksX* gene cluster in *B. subtilis* strains to remove KS domains from the *pksX* gene cluster and examined what was or was not produced by MALDI-TOF.<sup>6</sup>

Borriss and coworkers were also able to determine a similar sequence to the *pksX* gene cluster in *Bacillus amyloliquefaciens* FZB42, termed the *bae* cluster.<sup>7</sup> This cluster was missing one module compared to the *B. subtilis* strains previously mentioned. They deduced the bacillaene product by deleting the KS domain within *B. amyloliquefaciens* FZB 42 *bae* system, like the experiments of Chen et. al. They were unable to produce bacillaene, suggesting that bacillaene is produced by both the *pksX* and *bae* gene clusters.<sup>7</sup>

Difficidin was first discovered and isolated in 1987 by Zimmerman et. al.<sup>8</sup> Both it and oxydifficidin (Figure 6) were isolated from strains of *B. subtilis*. During this work, they were able to determine that these molecules had a broad-spectrum of antibiotic activity that works to inhibit protein biosynthesis *in vitro*, but the mechanism of action is still unknown.<sup>8</sup> In addition, Chen et. al was able to detect difficidin within *B. amyloliquefaciens* FZB42 through their methods and determined that difficidin was a

product of the *dif* gene cluster within this bacterium, which solidified that difficidin was produced by a *trans*-AT PKS.<sup>6</sup>

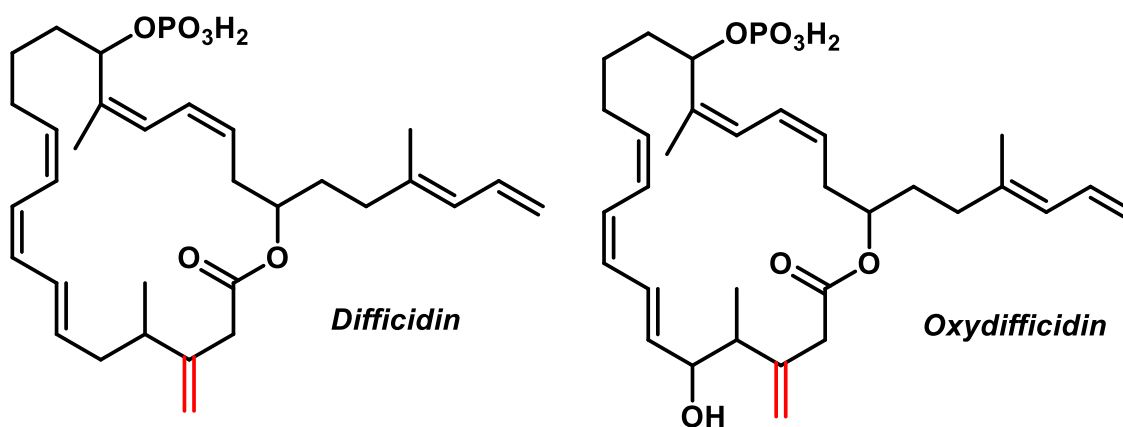


**Figure 6.** Difficidin and Oxydifficidin. The red bond indicates the abnormal  $\beta$ -branching.

The functionality and mode of action of difficidin, while yet to be fully explored, has been worked on within the last ten years. Borriss and co-workers worked on the functionality of this polyketide in terms of its antibacterial capabilities.<sup>9</sup> A disease called fire-blight disease is developed in apple and pear trees by the bacterium *Erwinia amylovora*.<sup>9</sup> Once infected, the bacterium begins to eat away at the plant, giving it a fiery appearance. Borriss and co-workers found that difficidin within *B. amyloliquefaciens* FZB42 and mutant strains were able to protect the plant from harm as a proactive measure.<sup>9</sup>

### 1.3 Previous Work of the Reddick Group

As mentioned previously, both bacillaene and difficidin from a structural perspective are unique and interesting. Bacillaene is a linear polyketide with an unusual methyl group (Figure 5) and difficidin is a cyclic polyketide with an unusual external

alkene (Figure 6). These  $\beta$ -branches are isomers. Since their genomes are known, the modules, and therefore the enzymes responsible for producing these unique  $\beta$ -branching patterns, can be determined. The work done by Ph.D. student Brittany Kiel looked at cloning copies of the enzymes, and ACPs from within a certain module necessary for the construction of the desired  $\beta$ -branch (Figure 7).

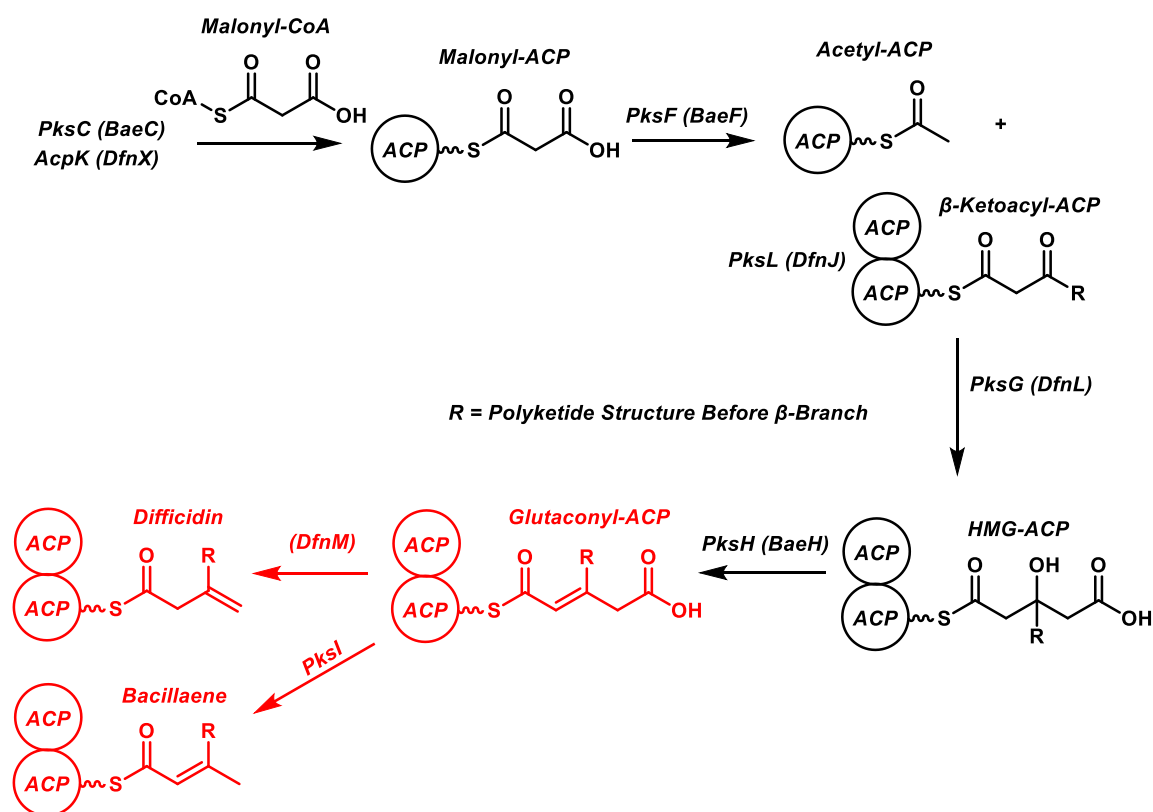


**Figure 7.** Synthesis of  $\beta$ -Branch in Bacillaene and Difficidin. *B. subtilis bacillaene genes (pks)* are next to *B. amylobiquefaciens difficidin genes (dfn)* in parenthesis. The section in red indicates the enzymatic processes in question.

These enzymes normally act on a complex polyketide intermediate structure attached to the ACP. Instead of trying to analyze this intermediate, Kiel worked with an acetoacetyl group, which contains the required  $\beta$ -keto group and makes it possible for the formation of the carbon-carbon bond to be catalyzed by these enzymes (Figure 8).

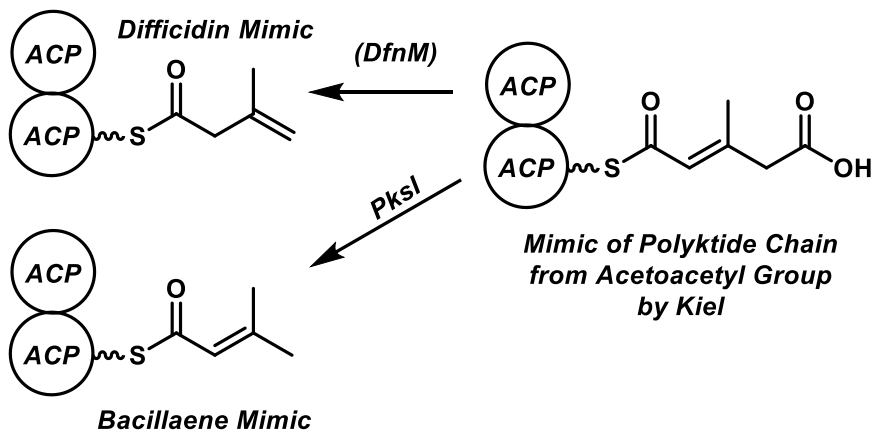


**Figure 8.** Work Accomplished by Brittany Kiel.

She then took the resulting mixture and analyzed it by mass spectrometry, which would give the mass of the product of the next step in the polyketide production process. The ultimate issue, however, is in analyzing the product of the *dfnX* gene cluster that deals with the unique  $\beta$ -branching pattern and comparing it to that of the *pksX* gene cluster. The mass of these two are identical, making it hard to verify which reaction is being accomplished onto the acetoacetyl group. Nuclear magnetic resonance was not possible during these experiments because trying to synthetically obtain these compounds of interest would be a feat within itself. More so, trying to analyze enzymes and desired products of these experiments would be nearly impossible by nuclear magnetic resonance simply due to the tumbling of the enzymes during analysis.

CHAPTER II  
SYNTHESIS OF POLYKETIDE STANDARDS

II.1 Present Works

Building from the work accomplished by the Reddick lab, this project seeks to develop internal standards to characterize the double bond nature of the mimics of intermediate products formed from the *dfnX* and *pksX* gene clusters. To accomplish this task, the goal would be to complete a set of coupling reactions known as 1-ethyl-3-(3-dimethylaminopropyl)carbodiimide (EDC) coupling to form the desired intermediates, compounds **3** and **6** (Figure 9) from the a carboxylic acid and a thiol.

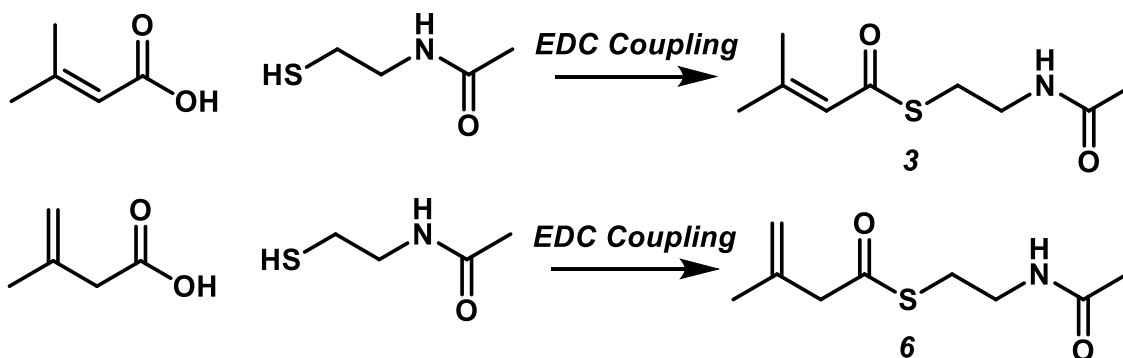


**Figure 9.** Simplified Reaction of Compound **3** and Compound **6**.

The general mechanism of an EDC coupling reaction between a carboxylic acid and a thiol, as seen in Figure 10, starts with an acid/base reaction between the carboxylic acid and the EDC. The resulting carboxylate does a nucleophilic attack onto the carbon of the EDC to form an interesting intermediate, but more importantly a good leaving group for the tetrahedral intermediate of the next step. Once the thiol does a nucleophilic attack

onto the carbonyl carbon to produce the tetrahedral intermediate, the carbonyl is then reformed and removed the byproduct urea and the product remains.

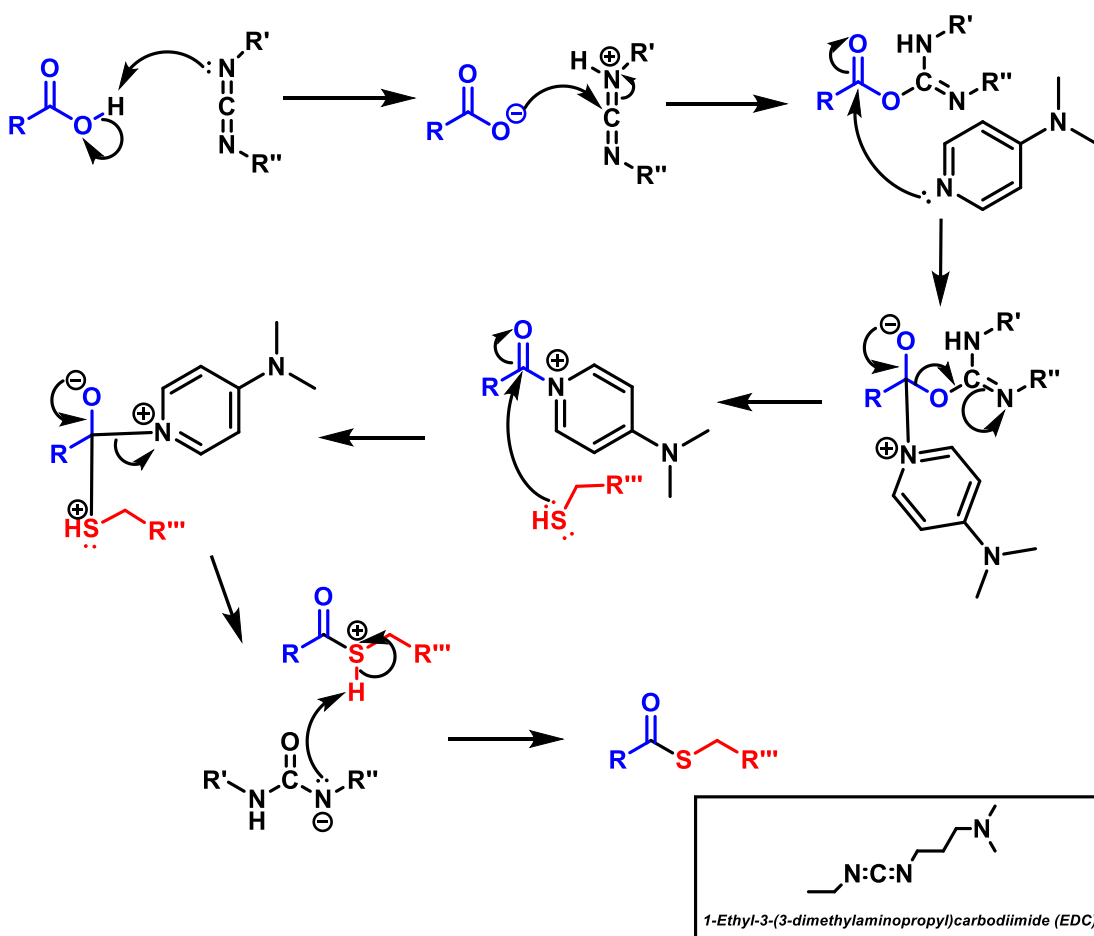


**Figure 10.** Proposed Mechanism for EDC Coupling Reaction. *The blue indicates the part of the final product from the carboxylic acid and the red indicates the part from the thiol.*

To begin this process, a test reaction was conducted to try to optimize reaction conditions. This was accomplished by adding 3-methyl-2-butenoic acid, **1**, and benzyl mercaptan to EDC in a reaction vessel under argon in dichloromethane while submerged in an ice bath. The other key reactant that was added to the reaction and is not present in Figure 10 is 4-dimethylaminopyridine (DMAP) which acts as another good

leaving group for the thiol during the step involving the collapse of the tetrahedral intermediate. The reaction was then allowed to stir for four hours in the ice bath and then brought back to room temperature over the course of twenty-four hours. Thus, compound **2** was produced with a 74% yield (Figure 11).

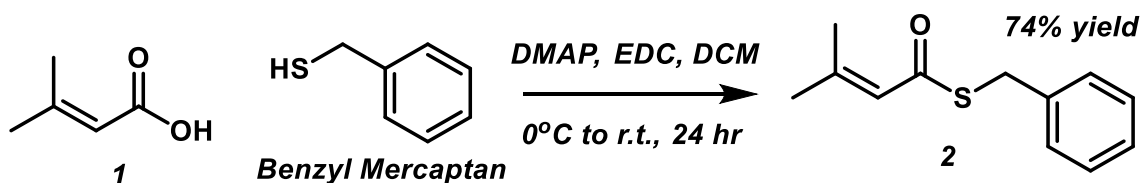


**Figure 11.** Test Reaction Between Compound **1** and Benzyl Mercaptan.

With this test reaction completed, the next steps were to begin the reactions of interest. To start, **1** and *N*-acetylcysteamine (SNAC) were added with EDC and DMAP under the same reaction conditions as those followed in the test reaction (Figure 12). The best results for this reaction yielded 84% of the desired product.

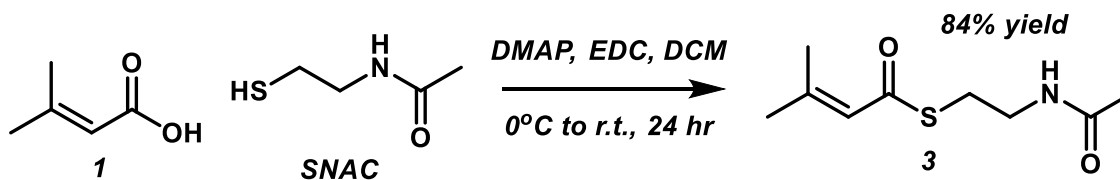


**Figure 12.** EDC Coupling Reaction Between Compound **1** and SNAC.

Unlike **1**, which was commercially available, 3-methyl-3-butenoic acid, **5**, was not; therefore, this had to be made synthetically before continuing to attempt the EDC coupling reaction to yield **6**. This was accomplished by a carboxylation reaction with the Grignard reagent chloro(2-methyl-2-propen-1-yl)-magnesium, **4**. The mechanism of this carboxylation reaction, as seen in Figure 13, shows the Grignard reagent more so acting

as a carbanion and a strong nucleophile to attach the carbon of the carbon dioxide to produce the carboxylate of the desired final product.

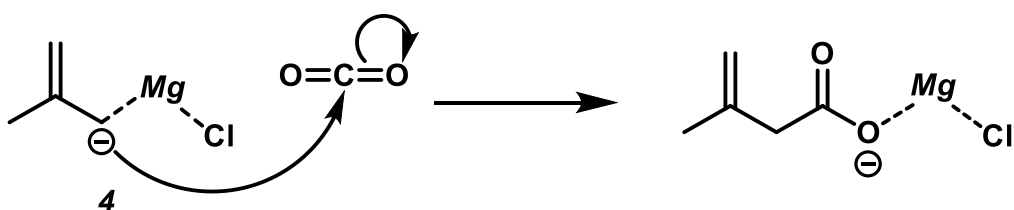


**Figure 13.** Proposed Mechanism for Carboxylation of Compound **4**.

The first attempts of forming compound **5**, which can be seen in Figure 14, was by reacting chloro(2-methyl-2-propen-1-yl)-magnesium, **4**, with dry ice under argon for ten minutes in a bath consisting of acetonitrile and dry ice to maintain a temperature of negative 41°C. The resulting mixture then underwent an acid/base extraction with 1 M ammonium chloride and 1 M sodium hydroxide to obtain the final product. With this procedure, this gave yields between 3% and 31%, which did not give enough material to continue to the EDC coupling reaction.

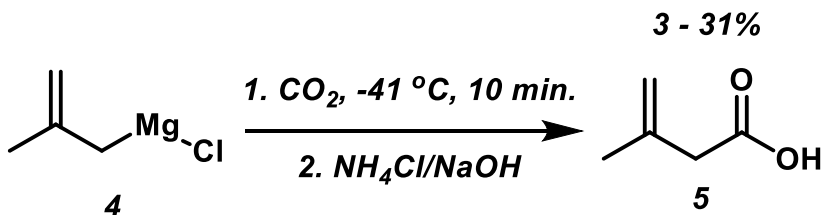


**Figure 14.** Carboxylation of Compound **4** with Ammonium Chloride and Sodium Hydroxide Workup.

Since this procedure was not providing enough material, a new reaction protocol was attempted. This involved adding the dry ice to a dry Erlenmeyer flask under atmosphere. Compound **4** was then added directly to the carbon dioxide and allowed to

react for thirty minutes, which was then followed by an acid/base reaction consisting of 5 M hydrochloric acid and 1 M sodium hydroxide (Figure 15). This procedure yielded 42% of **5** which was then immediately used in the EDC coupling reaction.

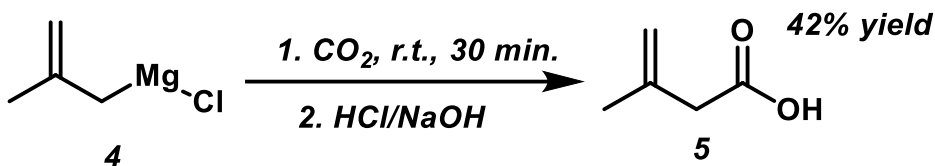


**Figure 15.** Carboxylation of Compound **4** with Hydrochloric Acid and Sodium Hydroxide Workup.

Interestingly, there were some reservations in using an acid/base extraction to obtain this final product as there being a possibility of isomerization to the more stable carboxylic acid, compound **1** (Figure 16). Compound **1** is more stable due to resonance between the tri-substituted alkene and the carboxylic acid which stabilizes the compound.

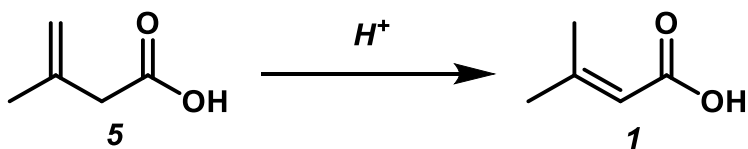


**Figure 16.** Isomerization of Compound **5** to Compound **1**.

During the extraction process of the second procedure, 5 M hydrochloric acid was used during the initial extraction and then to bring the pH of the aqueous layer down to a pH of 1 in the last extraction step and no isomerization was observed in the proton NMR.

With the necessary starting material now synthesized, the formation of **6** was performed with the same conditions used to form **3**. This was again accomplished by an EDC coupling reaction with **5**, SNAC and DMAP under argon at 0°C for four hours then

allowed to return to room temperature over the course of twenty-four hours (Figure 17).

The resulting compound **6** was formed at a 50% yield.

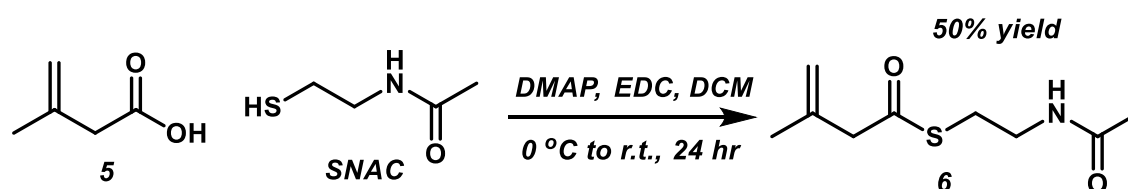


**Figure 17.** EDC Coupling Reaction Between Compound **5** and SNAC.

## II.2 Future Works and Conclusions

With the formation of these standards complete, the next step in the process will be to give these standards to a member of the Reddick group so they can take compounds **3** and **6** and the mimics of the polyketides that Brittany Kiel has worked with and submit them for gas chromatography mass spectrometry. This will produce fragmentation patterns for all the compounds. The predicted outcome is the fragmentation of compound **3** should correspond to that of the bacillaene mimic and the fragmentation of compound **6** should correspond to that of the difficidin mimic.

In terms of the reactions themselves, even though the goals of the project were accomplished by the formation of a sufficient amount of compound **3** and **6**, for further evaluation, it would be beneficial to improve upon the reaction conditions especially for the carboxylation reaction with Grignard reagent. Initially, this reaction was done under argon and carbon dioxide gas was bubbled into the system through a syringe. The Grignard reagent was dripped slowly into the reaction vessel where the carbon dioxide was bubbling. This resulted in the lowest yields of about 3 percent. When the dry ice was added directly to the system the yields increased slightly, but still were not enough to continue to the next step in the synthetic process. Finally, a new method was taken into

consideration and ultimately conducted which gave the best results so far of 42% yield. One of the biggest issues comes in the form of trying to minimize the amount of water present in the reaction. The dry ice must be crushed to help minimize the amount of water present in the reaction; however, it is inevitable with the present procedure that water will be present and, with Grignard reagents being highly reactive, exploring more options to conduct this reaction could be beneficial.

CHAPTER III  
HETEROCYCLE FORMATION INTRODUCTION MATERIAL

III.1 Isomerism and Chirality

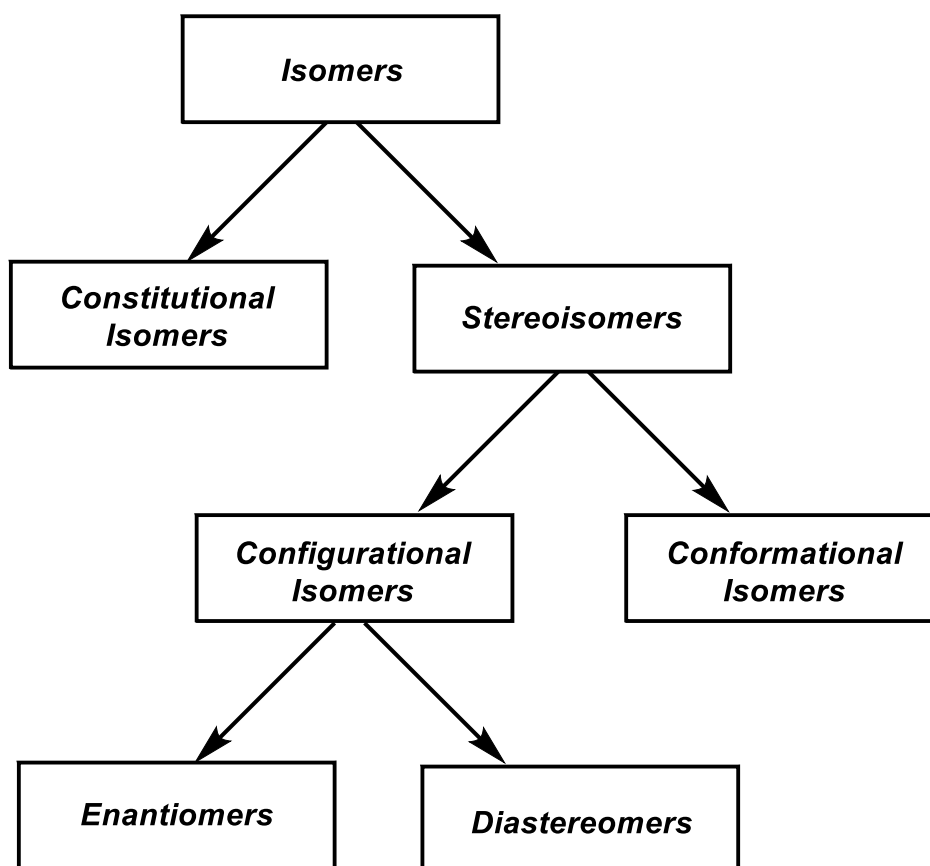
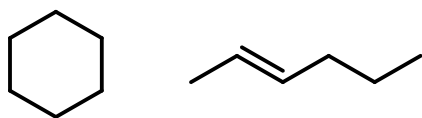


**Figure 18.** Flowchart of Isomerism.

Isomers are molecules that have the same molecular formula but have a distinct arrangement of atoms in space. A flowchart of isomerism can be seen in Figure 18.

Isomers can be further broken down into two categories: constitutional isomers and stereoisomers. Constitutional or structural isomers are molecules that have the same molecular formula but differ in structural formula. An example of this can be seen in cyclohexane and 2-hexene. They have the same molecular formula of  $C_6H_{12}$ , but one of their structural formulas is cyclic while the other is linear (Figure 19).



**Cyclohexane**      **2-Hexene**

**Figure 19.** Cyclohexane and 2-Hexene.

Stereoisomers are molecules that have the same structural formulas but differ in the spatial arrangement of the atoms themselves. An example of this is carvone. Carvone exists as a pair of molecules that have the same chemical structure but differ at one specific carbon, as seen in Figure 20.

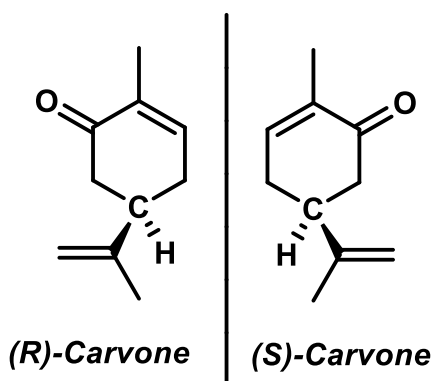


**Figure 20.** The Enantiomers of Carvone.

Stereoisomers can be further categorized as configurational isomers or conformational isomers. Configurational isomers are two molecules that cannot be

interconverted without breaking bonds. The example again can be seen in carvone (Figure 20). This pair of molecules cannot be overlapped without breaking the bonds located at the single carbon. Therefore, fundamentally, they have different configurations. Conformational isomers, however, are molecules that differ only by the angles about one or more sigma bonds. An example of this is butane. Looking at the Newman projections depicted in Figure 21, butane must overcome a rotational energy to achieve different conformations.

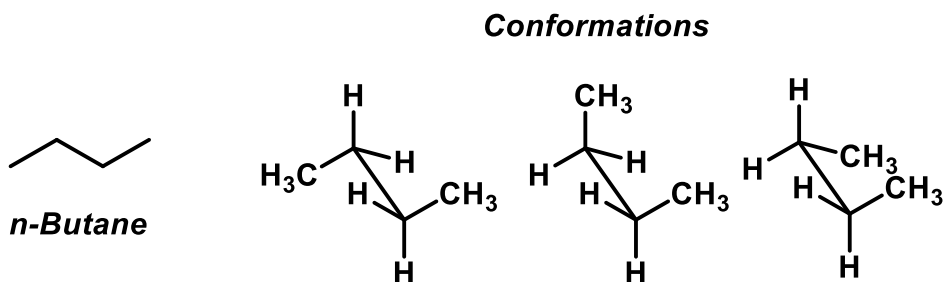


**Figure 21.** n-Butane and Newman Projections of n-Butane.

Finally, configurational isomers can be separated into enantiomers and diastereomers. An enantiomer is one of two stereoisomers that each exist as mirror images of each other and cannot be superimposed. Most amino acids exist as enantiomers, such as in L-valine in Figure 22. Valine exists as both L-valine and D-valine and there are enzymes that can interconvert these.

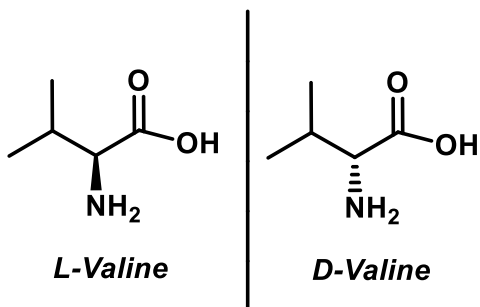


**Figure 22.** L-Valine and D-Valine.

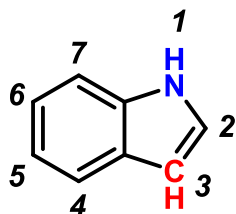
A diastereomer is one of two stereoisomers that are not mirror images and are non-superimposable. An example of this would be 2-bromo-3-chloro-butane. As seen in Figure 23, by changing where the bromine exists in space, these molecules are no longer mirror images of one another and they are non-superimposable.



**(R, R)-2-Bromo-3-Chloro-Butane**    **(S, R)-2-Bromo-3-Chloro-Butane**  
**Figure 23.** (R, R)-2-Bromo-3-Chloro-Butane and (S, R)-2-Bromo-3-Chloro-Butane.

### III.2 Indole-Containing Compounds

Indole's overall structure, which can be seen in Figure 24, is an aromatic, heterocyclic molecule containing a benzene and a pyrrole moiety. The compound has ten  $\pi$ -electrons participating in its aromaticity, which includes the nitrogen in the molecule.



**Indole**

**Figure 24.** Indole with Carbons Labelled.

Indoles will undergo electrophilic aromatic substitution at the most reactive site, the C-3 site, which can include aromatic nitration, aromatic halogenation, aromatic sulfonation, and alkylating Friedel-Crafts reactions.<sup>10</sup> However, electrophilic aromatic substitution can occur at the N-1 positions as well depending on the reagents used. Figure 25 shows two different reaction conditions for an alkylation at the N-1 and C-3 sites. Alkylation reactions with ionic salts tend to react with electrophiles at N-1 while organometallic compounds tend to react with electrophile at C-3. During these reactions, the resonance structure of the molecule allows for nucleophilic attack of an electrophile.<sup>11</sup> This is then followed by a tautomerization to reestablish resonance within the molecule.

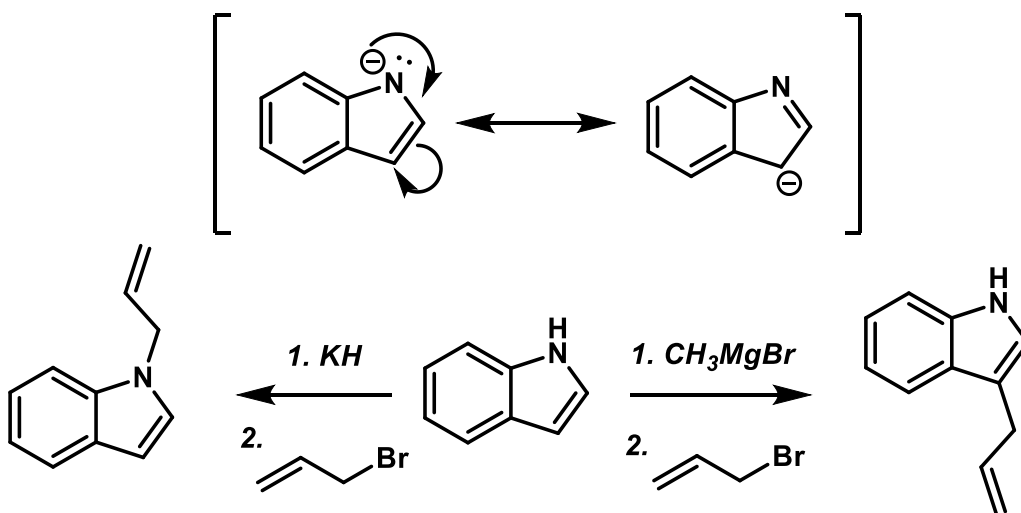
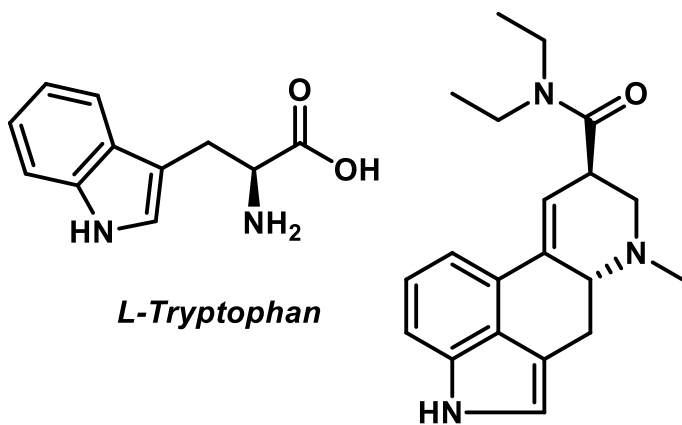


**Figure 25.** Resonance Structure of Indole and Alkylation at N-1 and C-3 of Indole.

Indoles and the indole moiety in general play an important role within biology, the simplest example being the amino acid L-tryptophan (Figure 26). Within humans, this molecule is known as an “essential” amino acid due to the body being unable to make it. This molecule must be taken in as part of the diet, which can typically be found within plant- and animal-based proteins. Ergot alkaloids also contain the indole moiety. Many of these types of natural products are produced by fungi from the genus *Claviceps* and are known to have hallucinogenic and neurologically damaging properties.<sup>12</sup> There are four main types of ergot alkaloids: clavines, lysergic acids, lysergic acid amides, and ergopeptides. A couple of the more infamous ergot alkaloids are lysergic acid diethylamide (LSD; Figure 26) and those produced by the *C. purpurea*, which caused major issues in the 1690s.<sup>12</sup>



***Lysergic Acid Diethylamide (LSD)***

**Figure 26.** L-Tryptophan and Lysergic Acid Diethylamide (LSD).

### III.3 Asymmetric Synthesis

Making molecules that are models or building blocks for natural products, such as the indoles mentioned, and even in terms of synthesizing novel drugs is key to understanding their utility, reactivity, and toxicity. Finding ways to do this synthetically is an area continuing to be explored, as many of these desired products are specific to one enantiomer and have a complex structure. Asymmetric synthesis is a tool that can be used to prepare these highly specific and complex products of interest.

Asymmetric synthesis, by IUPAC definition, is a chemical reaction where one or more new elements of chirality are formed in a substrate molecule and produces the stereoisomeric products in unequal amounts. There are a variety of methods that are categorized under the umbrella term asymmetric synthesis. One such method is known as enantioselective catalysis (Figure 27).<sup>13</sup> With this method, the starting material typically contains a prochiral aspect to it which can be converted from an achiral molecule to a chiral molecule in one step. This one step, in the case of enantioselective catalysis, is controlled by a chiral catalyst which will preferentially produce one enantiomer over the other. The benefit to this method is that all the starting material is utilized within the reaction; however, the final product is usually not purely the enantiomer being sought after and a way to analyze this phenomenon is known as enantiomeric excess (%ee). This is shown using the following equation,

$$\%ee = \frac{|Enantiomer\ 1 - Enantiomer\ 2|}{|Enantiomer\ 1 + Enantiomer\ 2|} \times 100$$

where the higher the percentage, the higher the purity of a single enantiomer obtained.

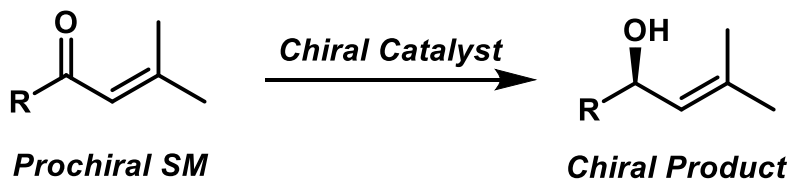


**Figure 27.** Enantioselective Catalysis Example.

A desymmetrization reaction modifies a symmetric molecule such that there is a loss of one or more symmetric elements in one step.<sup>14</sup> In the Petersen group, desymmetrization reactions (Figure 28) have been utilized to synthesize lactone derivatives from malonic esters via the use of a chiral Brønsted acid catalyst with good yields and %ee.

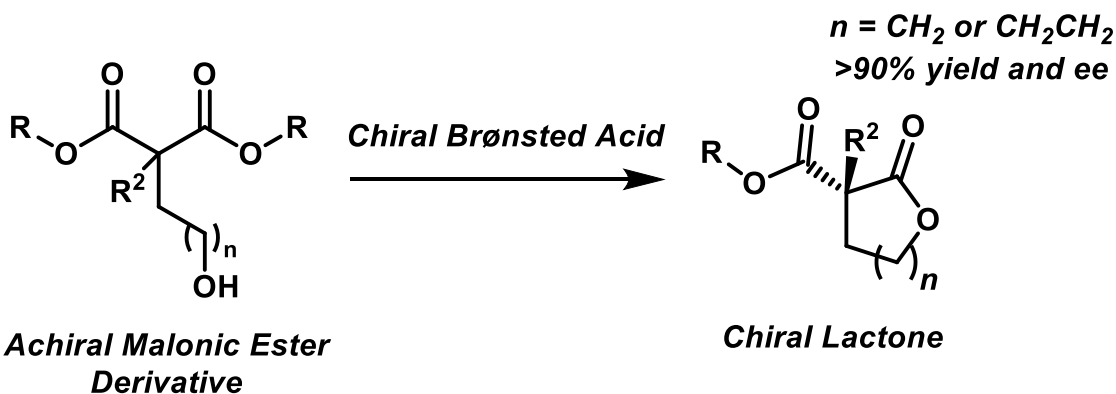


**Figure 28.** Formation of Chiral Lactones Via Desymmetrization of Malonic Ester Derivatives by Chiral Brønsted Acid.

This process has been accomplished by the cyclization of these malonic esters, which a proposed mechanism can be seen in Figure 29. The reaction starts with hydrogen bonding between the malonic acid and the Brønsted acid catalyst. The internal nucleophile, which is the hydroxyl group, attacks the carbonyl. This produces a tetrahedral intermediate and the protonated intermediate is deprotonated. The tetrahedral intermediate collapses and the alcohol is released. The protonated carbonyl

is then deprotonated to give the desired product. While this example does not utilize a chiral Brønsted acid catalyst, the concept is still the same. The final product of an achiral Brønsted acid will inherently be a mixture of both enantiomers as there is no stereoselectivity while the product of a chiral Brønsted acid will provide an enantioenriched product favoring one of the enantiomers over the other.

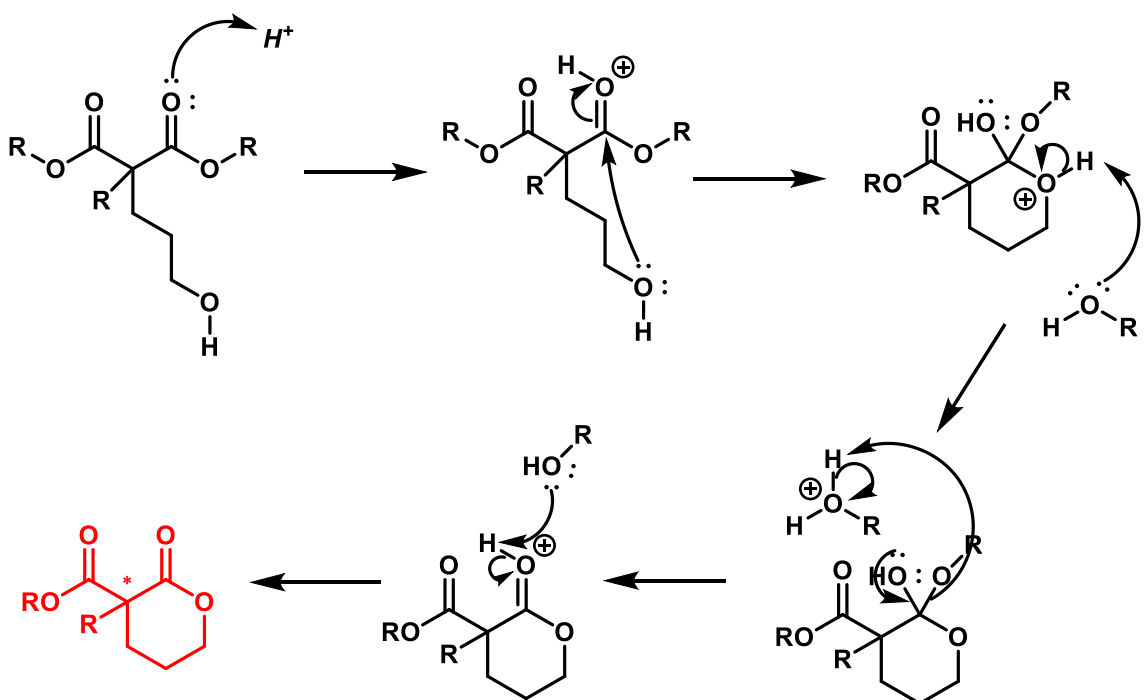


**Figure 29.** Proposed Mechanism for Achiral Brønsted Acid on Malonic Ester Derivative. The desired final product with the enantioenriched carbon is seen in red.

### III.4 Brønsted Acid Catalysts

Brønsted acids, in general, consist of any chemical species able to donate a proton. Some of the more common ones utilized as catalysts in the Petersen group include *p*-toluenesulfonic acid, methanesulfonic acid, and the axially chiral 3,3'-Bis(2,4,6-triisopropylphenyl)-1,1'-binaphthyl-2,2'-dihydrogen phosphate (TRIP). These catalysts can be seen in Figure 30.

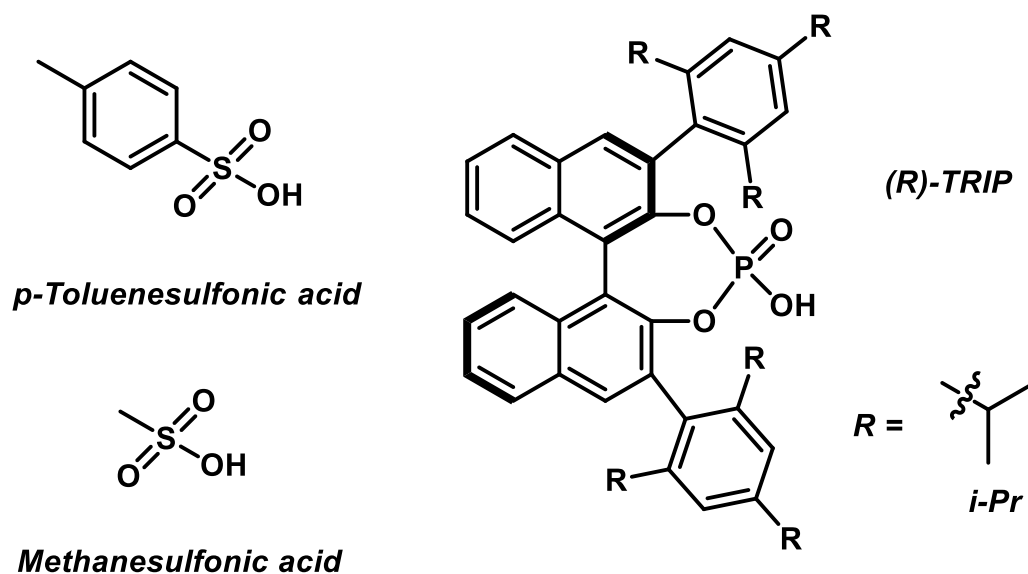


**Figure 30.** *p*-Toluenesulfonic Acid, Methanesulfonic Acid, and (*R*)-TRIP Catalyst.

*p*-Toluenesulfonic acid and methanesulfonic acid are achiral Brønsted acid catalysts and, therefore, will only produce a racemic mixture. If the goal of these desymmetrization reactions is to be stereoselective, then the use of a chiral catalyst such as the TRIP catalyst is required.

To achieve stereoselectivity, the TRIP catalyst has key characteristics that make it ideal to produce enantioenriched heterocyclic building blocks. First, the phosphoryl oxygens act as both a Brønsted acid and Brønsted base for hydrogen bonding interactions with the malonic ester. These interactions produce a complex between the chiral phosphoric acid and the malonic ester and promotes the cyclization through the proximity of the electrophilic carbon atom of the ester group and the nucleophilic oxygen atom of the hydroxyl group of the malonic acid (Figure 31).<sup>15</sup>

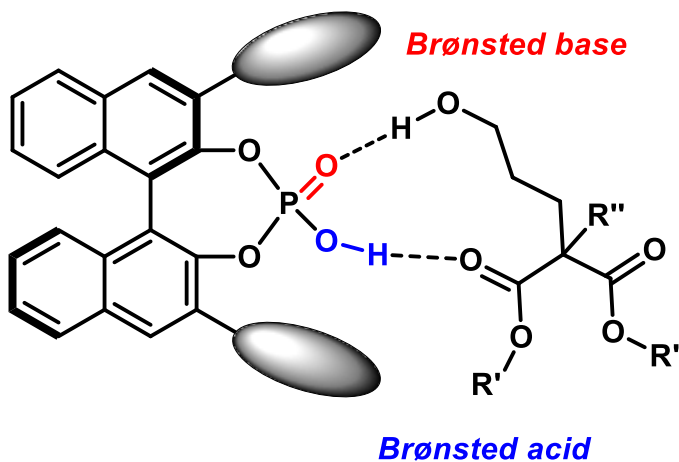


**Figure 31.** Proposed Activation Complex Between Malonic Ester and (*R*)-TRIP Catalyst.

Next, the 3,3' aryl groups of the TRIP catalyst act as stereo-controlling groups for the cyclization process.<sup>15</sup> Much like an enzyme binding pocket, only certain enantiomers of the malonic ester derivatives will be produced with the TRIP catalyst and provide steric hindrance to formation of the other enantiomers (Figure 31). Finally, the 1,1'-bi-2-naphthol (BINOL) backbone itself has an orientation, in the form of *R* or *S* enantiomers, which influences the directionality of the aryl groups and, therefore, the reactivity of the TRIP catalyst.<sup>15</sup>

### III.5 Previous Work of the Petersen Group

Dr. Jennifer Wilent of the Petersen group developed a novel asymmetric technique in which used malonic esters and produced enantioenriched lactone derivatives via desymmetrization. Primarily, her work focused on the synthesis of  $\gamma$ -lactones with high yields and enantioenrichment (Figure 32).<sup>16</sup>

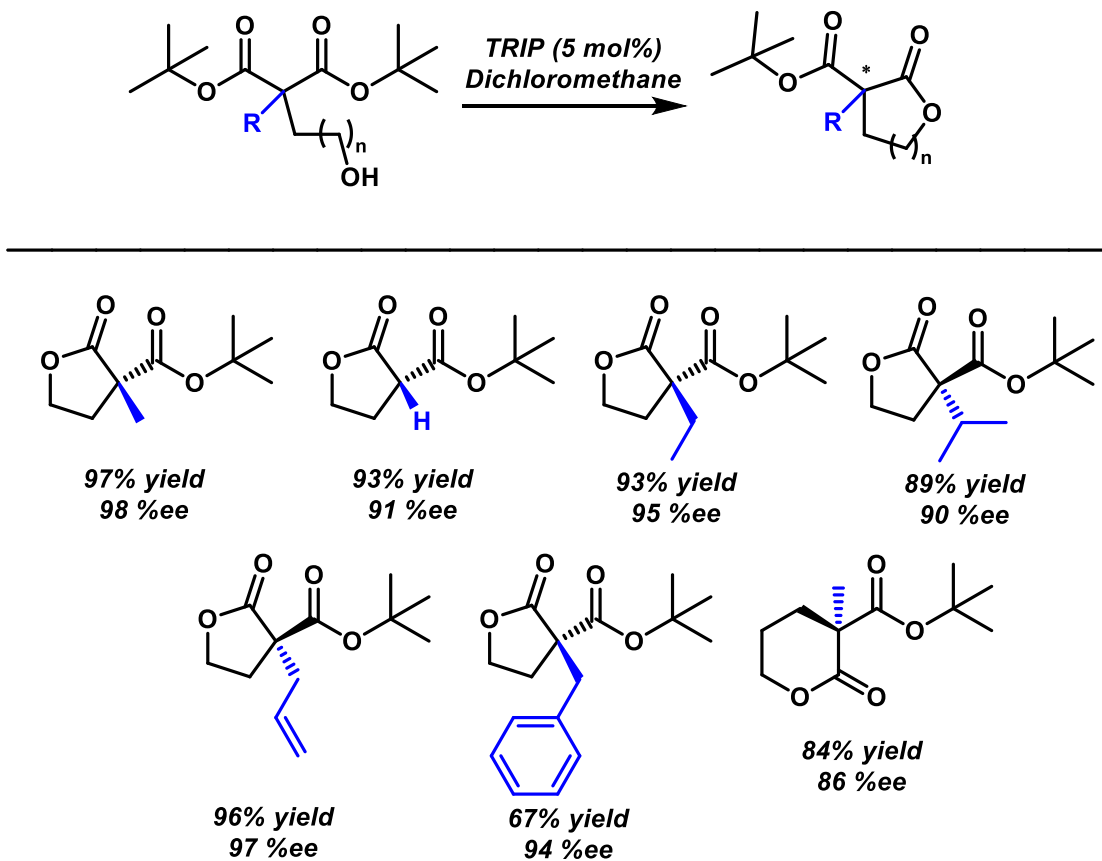


**Figure 32.** Work Accomplished by Jennifer Wilent.<sup>16</sup>

Current work in the Petersen group has expanded the scope of the methods developed by Dr. Wilent. Dr. Amber Kelley and graduate student Rhashanda Haywood, for example, furthered this work with interest in coumarin derivatives which came from the use of cyclic substrates in the desymmetrization reactions. The 3,4-dihydrocoumarin derivatives were produced in moderate to high yields and secondary alkyl groups did little to decrease the ee as the steric size increased (Figure 33).<sup>17</sup> In addition, carbon quaternary centers were able to be produced in both high yield and ee.

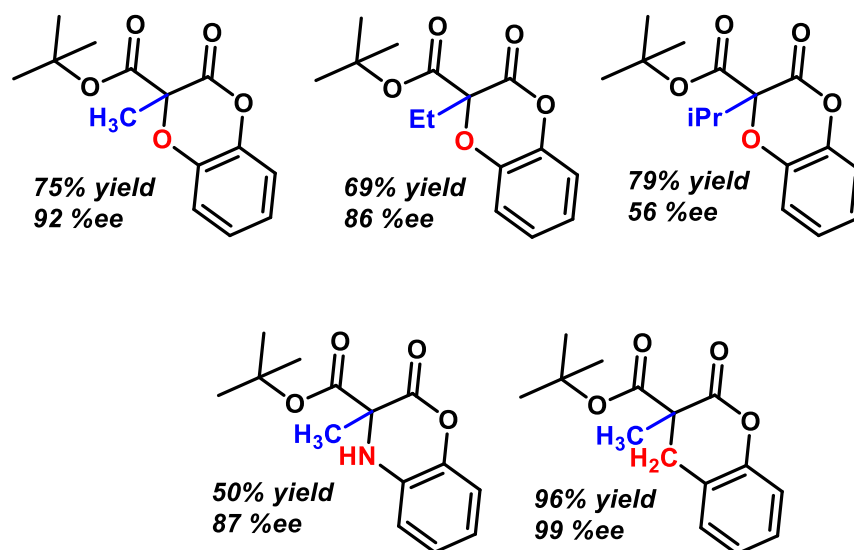
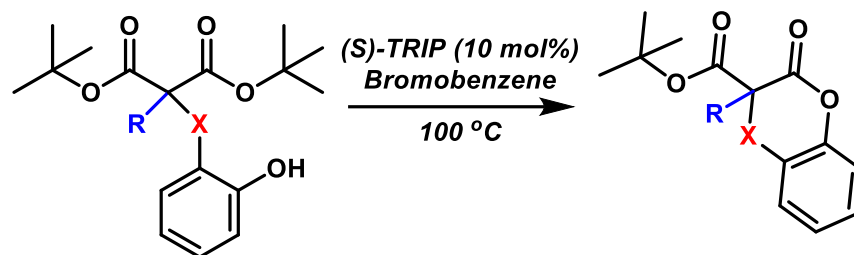


**Figure 33.** Work Accomplished by Amber Kelley.<sup>17</sup>

Dr. Tylisha Baber was able to take Dr. Wilent's work and apply it to a different starting material. Her interests lied in producing 6-membered lactones from dinitriles, which could be accomplished through a Pinner reaction.<sup>18</sup> The general reaction scheme can be seen in Figure 34. While the molecules were not enantioenriched, Dr. Baber obtained moderate yields with this novel asymmetric technique.

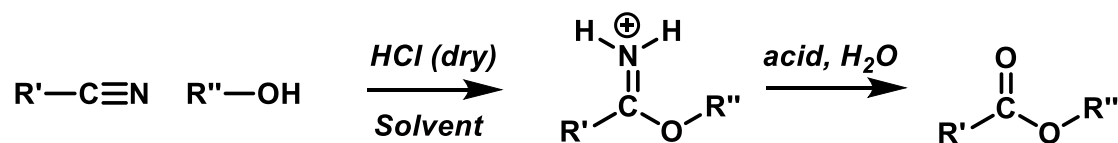


**Figure 34.** Pinner Reaction of Generic Nitrile and Alcohol.<sup>18</sup>

The formation of these 5- and 6-membered ring systems speaks to Dr. Wilent's work and the importance of it to synthesizing these building blocks. Future work in the Petersen group is focused on the preparation of alternative heterocyclic small molecules. Lactams would be an interesting route to go down as many compounds within biology contain them, one of the more iconic being penicillin. The issue with this is that nitrogen is not as nucleophilic as oxygen and so finding a strong enough nucleophile to attack the carbonyl carbon of a malonic ester would be difficult. Instead, pushing this work towards the formation of carbon-carbon bonds would potentially be novel and chemically significant.

CHAPTER IV  
SYNTHESIS OF ENANTIOENRICHED HETEROCYCLE THROUGH CARBON-CARBON  
BOND FORMATION

IV.1 Present Works

Building upon the previously mentioned research of the Petersen group, this project seeks to continue to expand on the stereoselective formation of heterocyclic building blocks by conducting a desymmetrization reaction to form a carbon-carbon bond and produce a new indole containing compound. Since the desired starting material, compound **8**, is not commercially available, it must be synthesized utilizing methods employed and developed by the Petersen group. To accomplish this, a proposed synthetic pathway, as well as the carbon-carbon bond of interest, has been mapped out in Figure 35. First, dimethyl malonate and indol-4-carboxyaldehyde (4-Indole) undergoes a Knoevenagel condensation to form compound **7**. Compound **7** then is reacted with palladium on carbon (Pd/C) and hydrogen gas to produce Compound **8**. Lastly, compound **8** undergoes an alkylation and then is cyclized via desymmetrization to produce compound **9** where the carbon-carbon bond is catalyzed, and the product is enantioenriched at the carbon indicated in Figure 35.

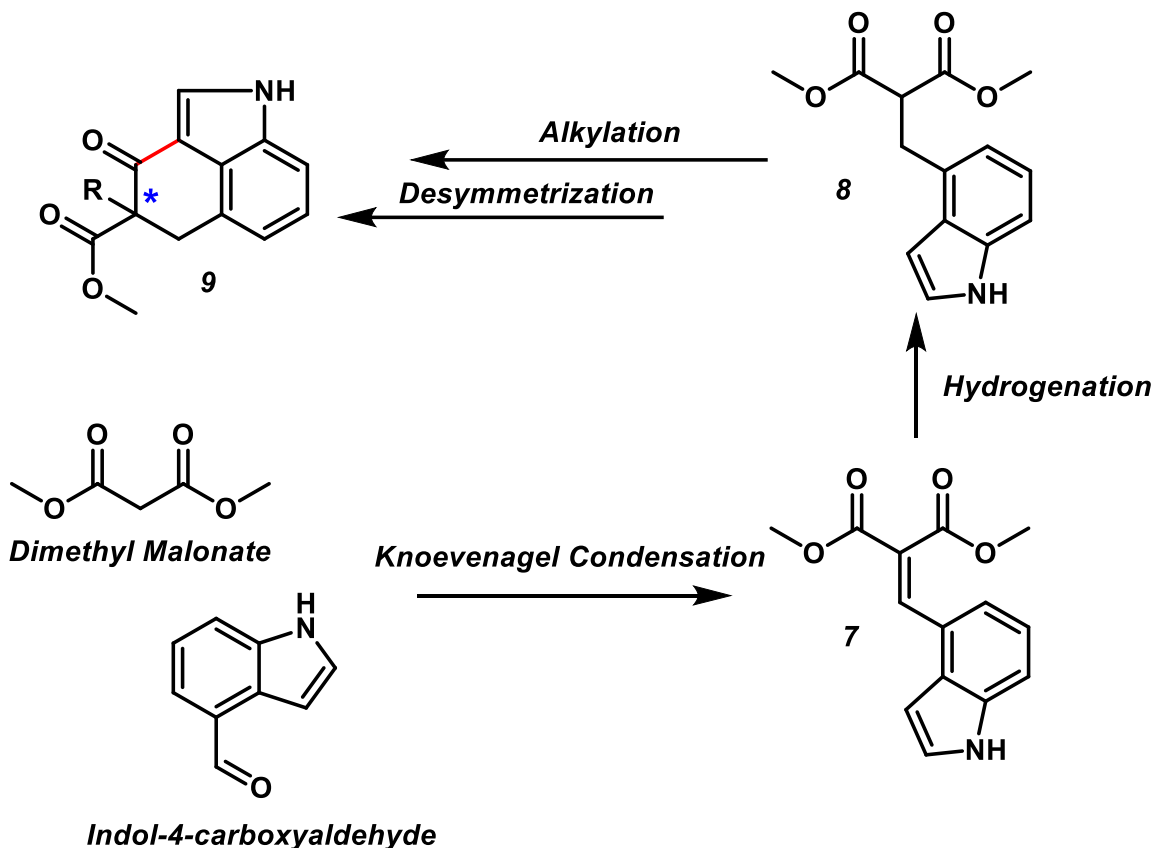


**Figure 35.** Proposed Synthetic Pathway to Form Compound 9. The carbon-carbon bond formed is in red and the desired enantioenriched carbon is marked with the blue star.

The general mechanism for a Knoevenagel condensation (Figure 36) begins with the malonic acid and another key reagent piperidine in an acid/base reaction. This produces a resonance structure with a strong nucleophilic carbon that attacks the carbonyl of the aldehyde. This produces a tetrahedral intermediate which the hydroxylate is then protonated by the piperidine. The following intermediate undergoes an elimination reaction to produce the desired product.

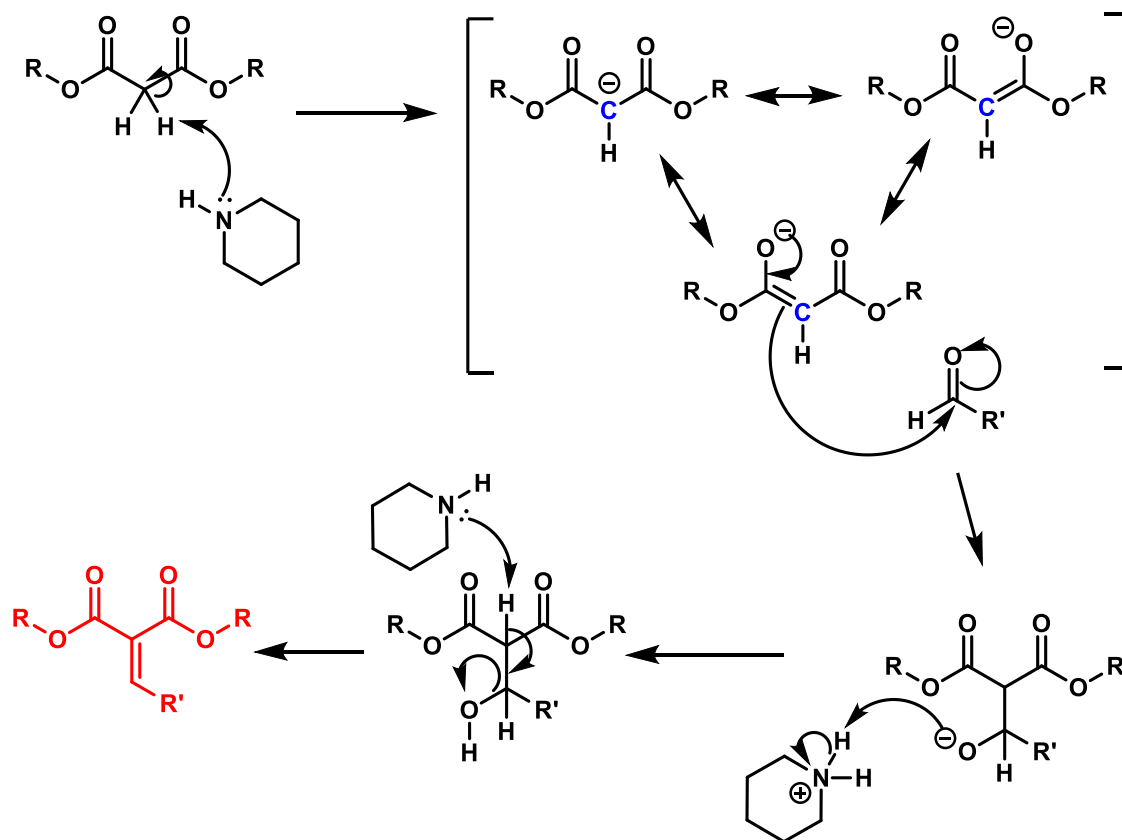


**Figure 36.** Proposed Mechanism of Knoevenagel Condensation Between Generic Malonate and Aldehyde in the Presence of Piperidine. *The nucleophilic carbon after deprotonation is shown in blue.*

As mentioned, starting with dimethyl malonate and 4-Indole, a Knoevenagel condensation was performed in the presence of piperidine and heat (Figure 37). Based on previous knowledge within the Petersen group, the appropriate temperature to use was right at the boiling point of the solvent used, which was toluene, and allowing the reaction to reflux. The resulting compound, **7**, was produced with a yield between 28% and 52%. This was easily identified by TLC visualization due to the new conjugation formed.

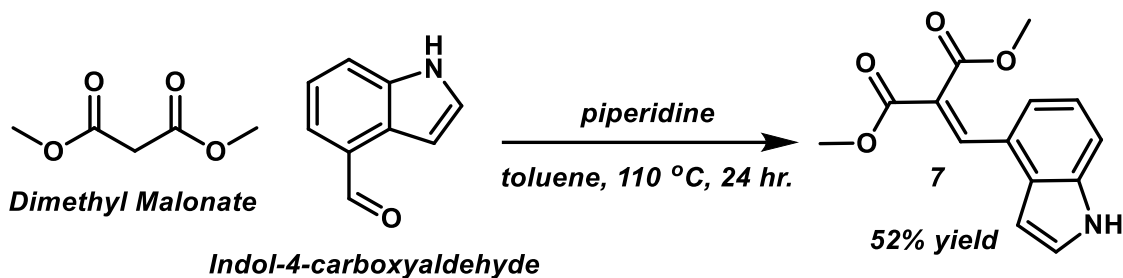


**Figure 37.** Knoevenagel Condensation Between Dimethyl Malonate and Indol-4-Carboxyaldehyde.

Following the formation of **7**, the next step in the process was to perform a hydrogenation reaction to reduce the central double bond. This was done to ensure a sole sigma bond to allow more flexibility for a potential cyclization. In addition, when the cyclization occurs, it is at this carbon that the enantioenrichment will occur. Compound **7** was added with palladium on carbon (Pd/C) and hydrogen gas was then introduced into the system (Figure 38). The reaction was then allowed to stir for twenty-four hours at room temperature and **8** was produced with a 58% yield.

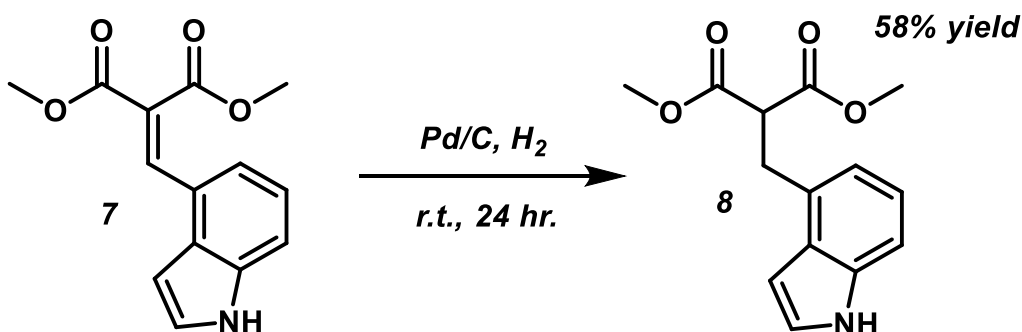


**Figure 38.** Hydrogenation of Compound **7**.

#### IV. Future Works and Conclusions

With the goal of the project to produce stereoselective, heterocyclic building blocks by conducting a desymmetrization reaction to form a carbon-carbon bond, the

last step in the process would be to attempt to cyclize compound **8** with a Brønsted acid catalyst and see if carbon-carbon bond formation is possible (Figure 39).

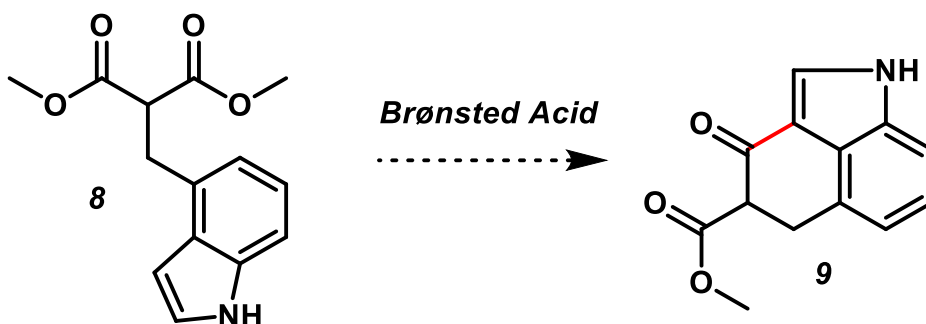


**Figure 39.** Desymmetrization of Compound **8** in the Presence of a Brønsted Acid.

Attempts have been made thus far with *p*-toluenesulfonic acid and increasing the temperature up to 80 °C, but no product formation was observed (Figure 40).

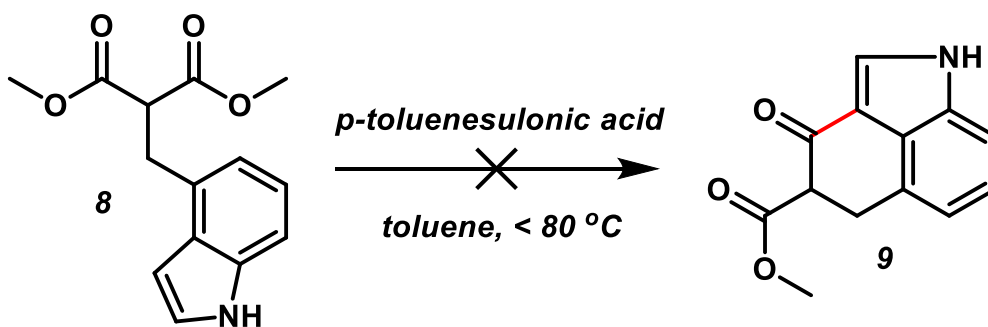


**Figure 40.** Attempt of Desymmetrization of Compound **8** in the Presence of *p*-Toluenesulfonic Acid.

Through the work accomplished by the Petersen group, it is known that these desymmetrization reactions are temperature and time dependent so varying the reaction conditions to allow the reaction to go to completion would be ideal. In addition, trying different Brønsted acid catalysts to see if cyclization is possible. Also, trying different solvents to obtain higher or lower temperatures could also prove to be beneficial. If this

is proven to be the case, using the TRIP catalyst to cyclize the product to obtain an enantioenriched heterocycle would be the following step. The potential issues with using this starting material, however, is the proton between the two carbonyl groups is still highly acidic. This can prove to be an issue with the cyclization process as this hydrogen could promote the reduction of the prochiral carbon into a  $sp^2$  hybridized carbon through decarboxylation of the ester (Figure 41), which would prevent enantioenrichment from occurring. Therefore, it would be beneficial to alkylate the starting material as well to reduce the acidity at that location.

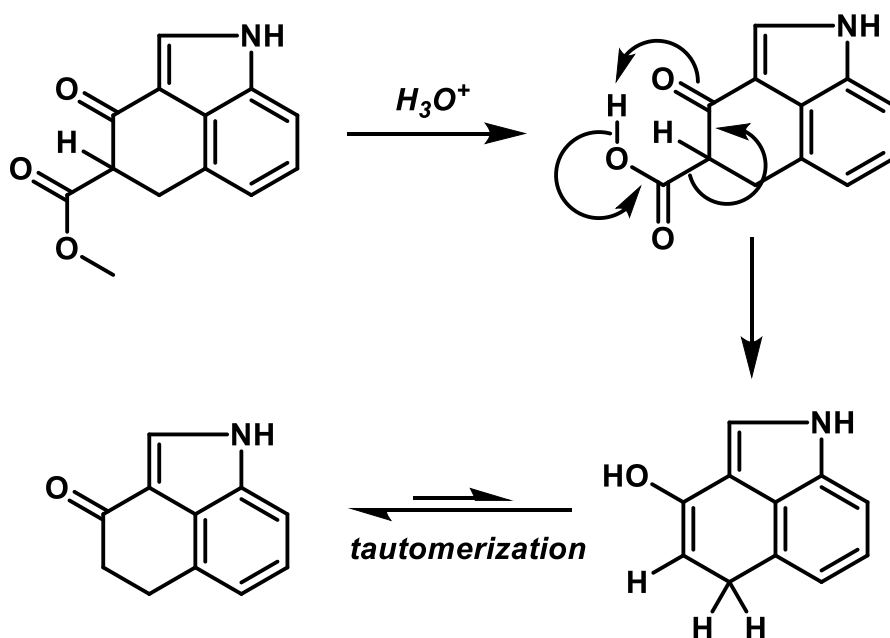
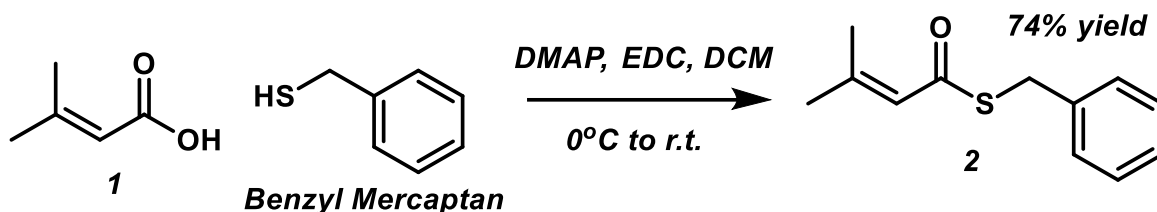


**Figure 41.** Decarboxylation of Compound 9.

CHAPTER V  
EXPERIMENTAL PROCEDURES AND RESULTS

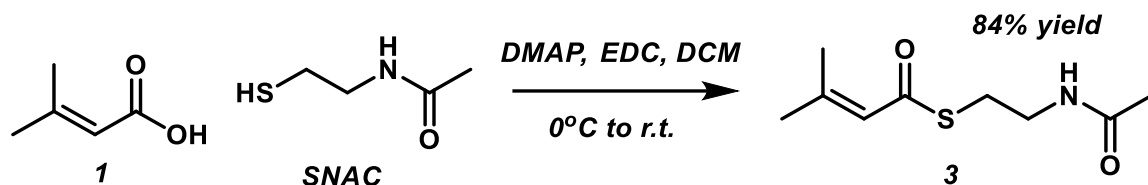
V.1 EDC Coupling of **1** and Benzyl Mercaptan



*N*-(1-Naphthyl)-ethylenediamine dihydrochloride (EDC; 520 mg, 2.0 mmol) was dissolved in dry dichloromethane (DCM; 15 mL) at 0 °C in a 50 mL flame dried round bottom flask under argon. 3,3'-Dimethylacrylic acid, **1**, (DAA; 203 mg, 2.0 mmol) and 4-dimethylaminopyridine (DMAP; 27.4 mg, 0.22 mmol) were added to the mixture and all materials were stirred until completely dissolved. To this mixture, benzyl mercaptan (0.210 mL, 1.7 mmol) was added slowly dropwise by syringe. The reaction was stirred at 0 °C for four hours, then allowed to return to room temperature and stirred for an additional twenty-four hours. The solvent was then evaporated, dried with magnesium sulfate (MgSO<sub>4</sub>), and the product was purified by column chromatography (Silica gel, 2:5 ethyl acetate:hexane), to yield compound **2** as a white solid (274 mg, 74% yield).

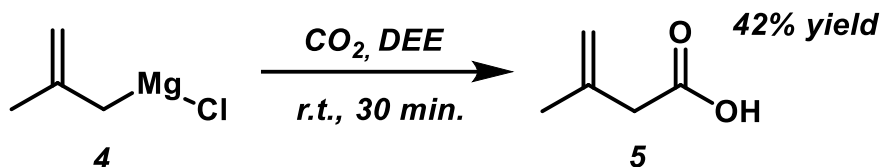
<sup>1</sup>H NMR (400 MHz, CDCl<sub>3</sub>) δ 7.30 (m, 5 H), 6.00 (s, 1 H), 4.16 (s, 2 H), 2.20 (s, 3 H), 1.87 (s, 3 H) ppm; HRMS (ESI): for C<sub>12</sub>H<sub>14</sub>OS[M+H]<sup>+</sup>: calculated 207.0838; found 207.0835

## V.2 EDC Coupling of 1 and SNAC



EDC (513 mg, 2.0 mmol) was dissolved in dry DCM (15 mL) at 0 °C in a 50 mL flame dried round bottom flask under argon. Compound **1** (199 mg, 2.0 mmol) and DMAP (24 mg, 0.20 mmol) were added to the mixture and all materials were stirred until completely dissolved. To this mixture, *N*-acetylcystamine (SNAC; 0.210 mL, 2.0 mmol) was added slowly dropwise via syringe. The reaction was stirred at 0 °C for four hours, then allowed to return to room temperature and stirred for an additional twenty-four hours. The solvent was then evaporated, and the product was purified by column chromatography (Silica gel, 2:5 ethyl acetate:hexane), to yield compound **3** as a white solid (334 mg, 84% yield). <sup>1</sup>H NMR (400 MHz, CDCl<sub>3</sub>) δ 5.99 (s, 1 H), 3.44 (q, *J* = 6.24 Hz, 2 H), 3.03 (t, *J* = 6.18 Hz, 2 H), 2.15 (s, 3 H), 1.94 (s, 3 H), 1.88 (s, 3 H) ppm; <sup>13</sup>C NMR (400 MHz, CDCl<sub>3</sub>) δ 189.6, 170.3, 155.1, 123.0, 40.1, 28.5, 27.4, 23.4, 21.4 ppm; HRMS (ESI): for C<sub>9</sub>H<sub>15</sub>O<sub>2</sub>SN[M+H]<sup>+</sup>: calculated 202.08963; found 202.08864

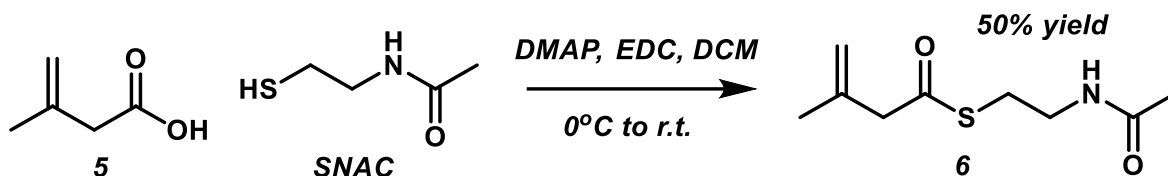
### V.3 Carboxylation of 2-Methylallylmagnesium Chloride



Dry ice (25 g) was crushed and then added to a flame dried 125 mL Erlenmeyer flask under atmospheric conditions and allowed to cool for five minutes. 2-Methylallylmagnesium chloride, **4**, (5.9 mL, 3.0 mmol) was bought commercially in a 0.5 M solution of tetrahydrofuran (THF) and added to the flask dropwise via syringe slowly. The reaction was stirred for thirty minutes until the dry ice had mostly reacted or sublimed. The reaction vessel was then submerged into a bath of room temperature water to allow the dry ice to completely sublime. The Erlenmeyer flask was then removed from the water bath and dry diethyl ether (DEE; 10 mL) was added to the flask. The mixture was then quenched with hydrochloric acid (5 M, 10 mL) and the aqueous layer was extracted twice with dry DEE (10 mL each). The combined organic layers were then placed into a separatory funnel and a sodium hydroxide solution was added (1 M, 10 mL). The layers were then shaken and separated. The basic aqueous layer was rinsed twice with dry DEE (10 mL each) and the organic layers were set aside. Hydrochloric acid (5M) was then added to the aqueous layer until the pH of the mixture was below two. The aqueous layer was then extracted twice with dry DEE (15 mL each) and the organic layers were then combined, dried over MgSO<sub>4</sub>, filtered, and evaporated to yield compound **5** as a dark yellow oil (125 mg, 42% yield). *Caution! Potential high volatility.*

<sup>1</sup>H NMR (400 MHz, CDCl<sub>3</sub>) δ 4.85 (s, 1 H), 4.80 (s, 1 H), 2.98 (s, 2 H), 1.75 (s, 3 H) ppm

#### V.4 EDC Coupling of **5** and SNAC



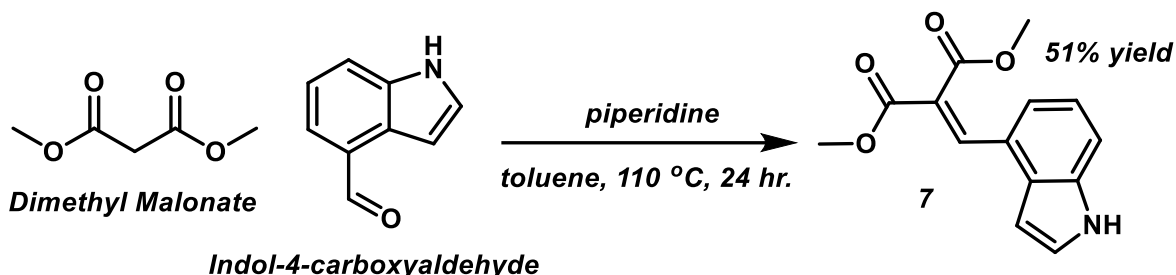
EDC (258 mg, 1.0 mmol) was dissolved in dry DCM (15 mL) at 0 °C in a 50 mL flame dried round bottom flask under argon. Compound **5** (100 mg, 1.0 mmol) and DMAP (20.3 mg, 0.166 mmol) were added to the mixture and all materials were stirred until completely dissolved. To this mixture, SNAC (0.14 mL, 1.3 mmol) was added dropwise. The reaction was stirred at 0 °C for four hours, then allowed to return to room temperature and stirred for an additional twenty-four hours. The solvent was then evaporated, and the product was purified by column chromatography (Silica gel, 0.1% triethyl amine, 2:5 ethyl acetate:hexane) to yield compound **6** as a light yellow oil (100 mg, 50% yield). *Caution! Possilbe isomerization of material to compound **3** during purification.*

$^1\text{H}$  NMR (400 MHz,  $\text{CDCl}_3$ )  $\delta$  4.93 (s, 1 H), 4.87 (s, 1 H), 3.39 (q,  $J = 6.15$ , 2 H), 3.23 (s, 2 H), 2.99 (t,  $J = 6.52$ , 2 H), 2.00 (s, 3 H), 1.93 (s, 3 H) ppm;  $^{13}\text{C}$  NMR (400 MHz,  $\text{CDCl}_3$ )  $\delta$  197.80, 171.29, 138.23, 116.20, 52.78, 39.72, 28.66, 23.17, 22.46 ppm; HRMS (ESI): for  $\text{C}_9\text{H}_{15}\text{O}_2\text{SN}[\text{M}+\text{H}]^+$ : calculated 202.08963; found 202.08959

*Purity: 77% of compound **6** and 23% of compound **3** present as determined by GC.*

### V.5 Knoevenagel Condensation of Dimethyl Malonate and Indol-4-

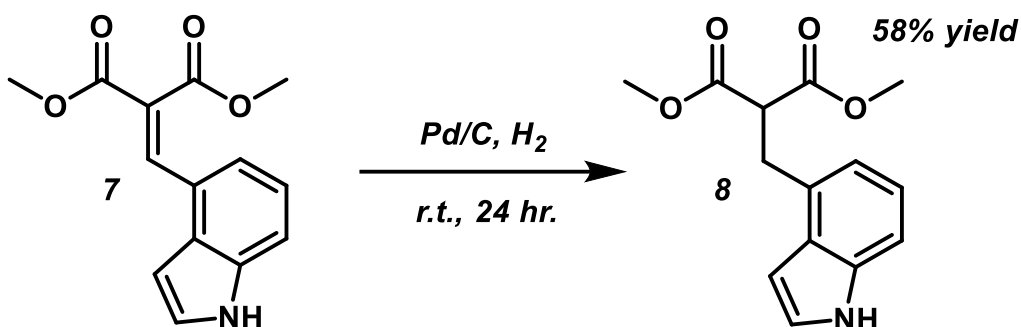
carboxyaldehyde



Indol-4-carboxyaldehyde (4-Indole; 302 mg, 2.1 mmol) was dissolved in dry toluene (10 mL) in a 50 mL flame dried two-necked round bottom flask. A condenser was added to the flask and the vessel was filled with argon. To the round bottom flask, dimethyl malonate (DMM; .235 mL, 2.0 mmol) was added. Piperidine (.011 mL; .011 mmol) was added to the reaction vessel dropwise and the mixture was inserted into an oil bath and stirred under reflux for twenty-four hours. The vessel was then removed from the bath and the solvent was evaporated. The mixture was purified by column chromatography (Silica Gel, 2:5 ethyl acetate:hexane) to yield compound **7** as a bright yellow oil (272 mg, 51% yield).

$^1\text{H}$  NMR (400 MHz,  $\text{CDCl}_3$ )  $\delta$  7.44 (d,  $J = 8.01$  Hz, 1 H), 7.30 (t,  $J = 2.94$  Hz, 1 H), 7.24 (t,  $J = 3.68$  Hz, 1 H), 7.16 (t,  $J = 7.78$  Hz, 1 H), 6.72 (m, 1 H), 3.87 (s, 3 H), 3.80 (s, 3H) ppm;  $^{13}\text{C}$  NMR (400 MHz,  $\text{CDCl}_3$ )  $\delta$  167.77, 166.97, 141.34, 136.01, 128.48, 125.25, 124.96, 124.87, 122.10, 119.76, 113.79, 100.98, 57.76, 57.74 ppm; HRMS (ESI): for  $\text{C}_{14}\text{H}_{12}\text{O}_4\text{N}[\text{M}+\text{H}]^+$ : calculated 282.07368; found 282.07298

#### V.6 Hydrogenation of 7



Palladium on carbon (Pd/C; 26 mg; .24 mmol) was added to a 50 mL flame dried round bottom flask. Compound **7** (268 mg; 1.0 mmol) was dissolved in ethyl acetate (10 mL) and added to the round bottom flask. The flask was sealed with a septum and the mixture was stirred. A vacuum was introduced into the system until bubbles appeared in the bottom of the flask. The vacuum was then removed, and a hydrogen gas source was introduced for about five seconds. The hydrogen gas source was removed from the vessel and the vacuum was reintroduced into the system. This was repeated two more times and ended with the hydrogen gas source being inserted into the reaction vessel and allowing it to stir for twenty-four hours. The mixture was then filtered, dried over MgSO<sub>4</sub>, and the solvent was evaporated to produce compound **8** as a purple solid (156 mg, 58% yield).

<sup>1</sup>H NMR (400 MHz, CDCl<sub>3</sub>) δ 7.27 (d, *J* = 8.24 Hz, 1 H), 7.20 (t, *J* = 2.91 Hz, 1 H), 7.09 (t, *J* = 7.62 Hz, 1 H), 6.93 (d, *J* = 7.10 Hz, 1 H), 6.58 (m, 1 H), 3.88 (t, *J* = 7.72 Hz, 1 H), 3.68 (s, 6H), 3.52 (d, *J* = 7.67 Hz, 2 H) ppm; <sup>13</sup>C NMR (400 MHz, CDCl<sub>3</sub>) δ 169.71, 169.52, 135.83, 129.80, 124.16, 122.17, 119.92, 110.02, 100.68, 52.77, 52.72, 52.67, 32.62 ppm; HRMS (ESI): for C<sub>14</sub>H<sub>14</sub>O<sub>4</sub>N[M+H]<sup>+</sup>: calculated 262.1074; found 262.1069

## REFERENCES

- 1 Keatinge-Clay, A. T. The Structures of Type I Polyketide Synthases. *Nat. Prod. Rep.* **2012**, 29 (10), 1050. <https://doi.org/10.1039/c2np20019h>.
- 2 Helfrich, E. J. N.; Piel, J. Biosynthesis of Polyketides by Trans-AT Polyketide Synthases. *Nat. Prod. Rep.* **2016**, 33 (2), 231–316. <https://doi.org/10.1039/C5NP00125K>.
- 3 Piel, J. Biosynthesis of Polyketides by Trans-AT Polyketide Synthases. *Nat. Prod. Rep.* **2010**, 27 (7), 996. <https://doi.org/10.1039/b816430b>.
- 4 Dorrestein, P. C.; Bumpus, S. B.; Calderone, C. T.; Garneau-Tsodikova, S.; Aron, Z. D.; Straight, P. D.; Kolter, R.; Walsh, C. T.; Kelleher, N. L. Facile Detection of Acyl and Peptidyl Intermediates on Thiotemplate Carrier Domains via Phosphopantetheinyl Elimination Reactions during Tandem Mass Spectrometry. *Biochemistry* **2006**, 45 (42), 12756–12766. <https://doi.org/10.1021/bi061169d>.
- 5 Calderone, C. T.; Kowtoniuk, W. E.; Kelleher, N. L.; Walsh, C. T.; Dorrestein, P. C. Convergence of Isoprene and Polyketide Biosynthetic Machinery: Isoprenyl-S-Carrier Proteins in the PksX Pathway of *Bacillus Subtilis*. *Proceedings of the National Academy of Sciences* **2006**, 103 (24), 8977–8982. <https://doi.org/10.1073/pnas.0603148103>.
- 6 Chen, X.-H.; Vater, J.; Piel, J.; Franke, P.; Scholz, R.; Schneider, K.; Koumoutsi, A.; Hitzeroth, G.; Grammel, N.; Strittmatter, A. W.; Gottschalk, G.; Süssmuth, R. D.; Borriss, R. Structural and Functional Characterization of Three Polyketide Synthase Gene Clusters in *Bacillus Amyloliquefaciens* FZB 42. *JB* **2006**, 188 (11), 4024–4036. <https://doi.org/10.1128/JB.00052-06>.

- 7 Chen, X. H.; Koumoutsis, A.; Scholz, R.; Schneider, K.; Vater, J.; Süssmuth, R.; Piel, J.; Borriss, R. Genome Analysis of *Bacillus Amyloliquefaciens* FZB42 Reveals Its Potential for Biocontrol of Plant Pathogens. *Journal of Biotechnology* **2009**, *140* (1–2), 27–37. <https://doi.org/10.1016/j.jbiotec.2008.10.011>.
- 8 Zimmerman, S. B.; Schwartz, C. D.; Monaghan, R. L.; Pelak, B. A.; Weissberger, B.; Gilfillan, E. C.; Mochales, S.; Hernandez, S.; Currie, S. A.; Tejera, E.; Stapley, E. O. Difficidin and Oxydifficidin: Novel Broad Spectrum Antibacterial Antibiotics Produced by *Bacillus Subtilis*. I. Production, Taxonomy and Antibacterial Activity. *J. Antibiot.* **1987**, *40* (12), 1677–1681. <https://doi.org/10.7164/antibiotics.40.1677>.
- 9 Müller, S.; Strack, S. N.; Hoefler, B. C.; Straight, P. D.; Kearns, D. B.; Kirby, J. R. Bacillaene and Sporulation Protect *Bacillus Subtilis* from Predation by *Myxococcus Xanthus*. *Appl. Environ. Microbiol.* **2014**, *80* (18), 5603–5610. <https://doi.org/10.1128/AEM.01621-14>.
- 10 Bartoli, G.; Bencivenni, G.; Dalpozzo, R. Organocatalytic Strategies for the Asymmetric Functionalization of Indoles. *Chem. Soc. Rev.* **2010**, *39* (11), 4449. <https://doi.org/10.1039/b923063g>.
- 11 Lakhdar, S.; Westermaier, M.; Terrier, F.; Goumont, R.; Boubaker, T.; Ofial, A. R.; Mayr, H. Nucleophilic Reactivities of Indoles. *J. Org. Chem.* **2006**, *71* (24), 9088–9095. <https://doi.org/10.1021/jo0614339>.
- 12 Corbett, K.; Dickerson, A. G.; Mantle, P. G. Metabolic Studies on *Claviceps Purpurea* during Parasitic Development on Rye. *Journal of General Microbiology* **1974**, *84* (1), 39–58. <https://doi.org/10.1099/00221287-84-1-39>.
- 13 Bolm, C.; Gladysz, J. A. Introduction: Enantioselective Catalysis. *Chem. Rev.* **2003**, *103* (8), 2761–2762. <https://doi.org/10.1021/cr030693c>.

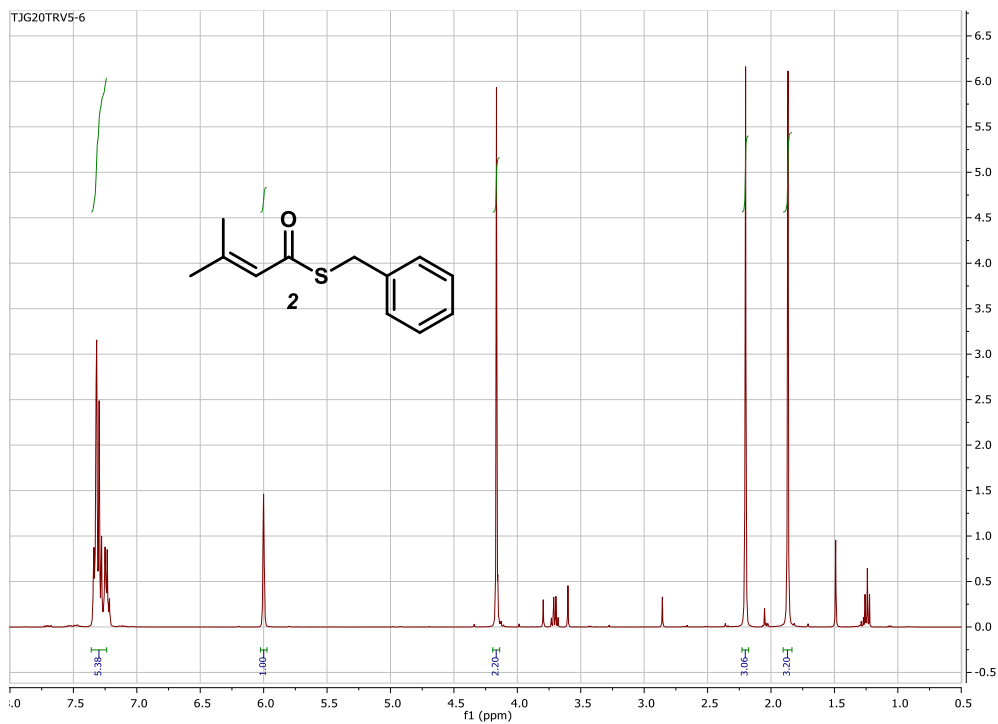
- 14 Auf der heyde, T. P. E.; Buda, A. B.; Mislow, K. Desymmetrization and Degree of Chirality. *J Math Chem* **1991**, 6 (1), 255–265.  
<https://doi.org/10.1007/BF01192584>.
- 15 Rajat, M.; Mallojjala, S. C.; Wheeler, S. E. Chiral Phosphoric Acid Catalysis: From Numbers to Insights *Chem Soc Rev.* **2018**, 47 (4), 1142-1158.  
<http://doi.org/10.1039/c6cs00475j>
- 16 Wilent, J.; Petersen, K. S. Enantioselective Desymmetrization of Diesters. *J. Org. Chem.* **2014**, 79 (5), 2303–2307. <https://doi.org/10.1021/jo402853v>.
- 17 Kelley, A. M.; Haywood, R. D.; White, J. C.; Petersen, K. S. Enantioselective Desymmetrizations of Diesters to Synthesize Fully Substituted Chiral Centers of 3,4-Dihydrocoumarins and Related Compounds. *ChemistrySelect* **2020**, 5, 3018–3022. <https://doi.org/10.1021/jo402853v>.
- 18 Baber, T. A Novel Application of Organocatalysis for the Synthesis of Six-Membered Ring Lactones. M.S. Thesis, University of North Carolina at Greensboro, Greensboro, NC, 2019.

## APPENDIX A.

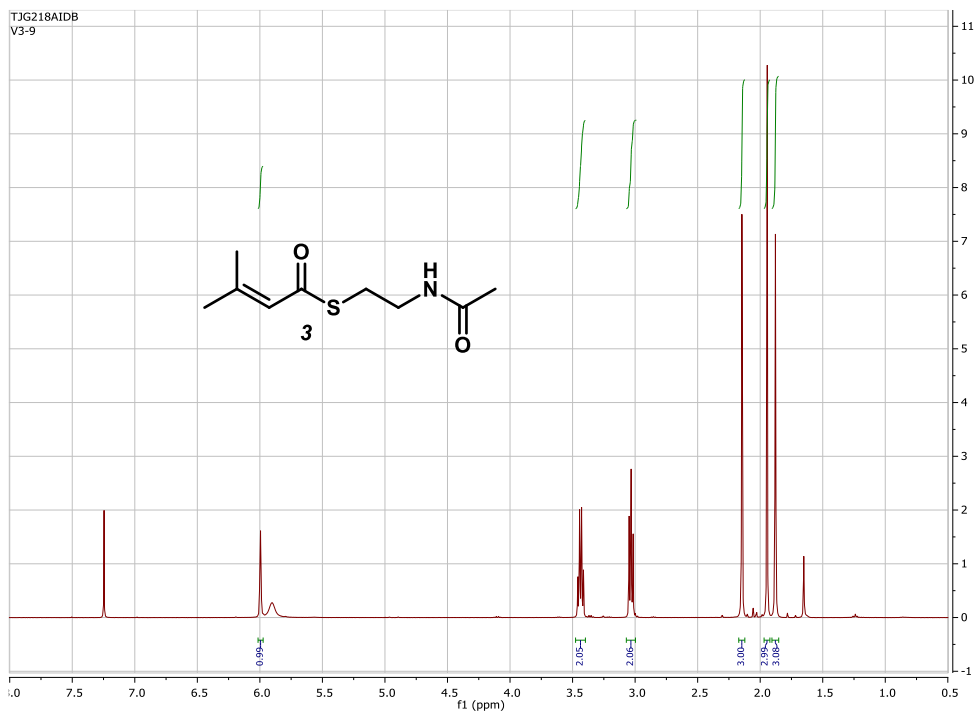
### NMR Spectra

The  $^1\text{H}$  and  $^{13}\text{C}$  nuclear magnetic resonance (NMR) spectra were plotted on 400 MHz spectrometer using  $\text{CDCl}_3$  as a solvent at room temperature. The NMR chemical shifts ( $\delta$ ) are reported in ppm. Abbreviations for  $^1\text{H}$  NMR: s = singlet, d = doublet, m = multiplet, b = broad, t = triple, q = quartet.

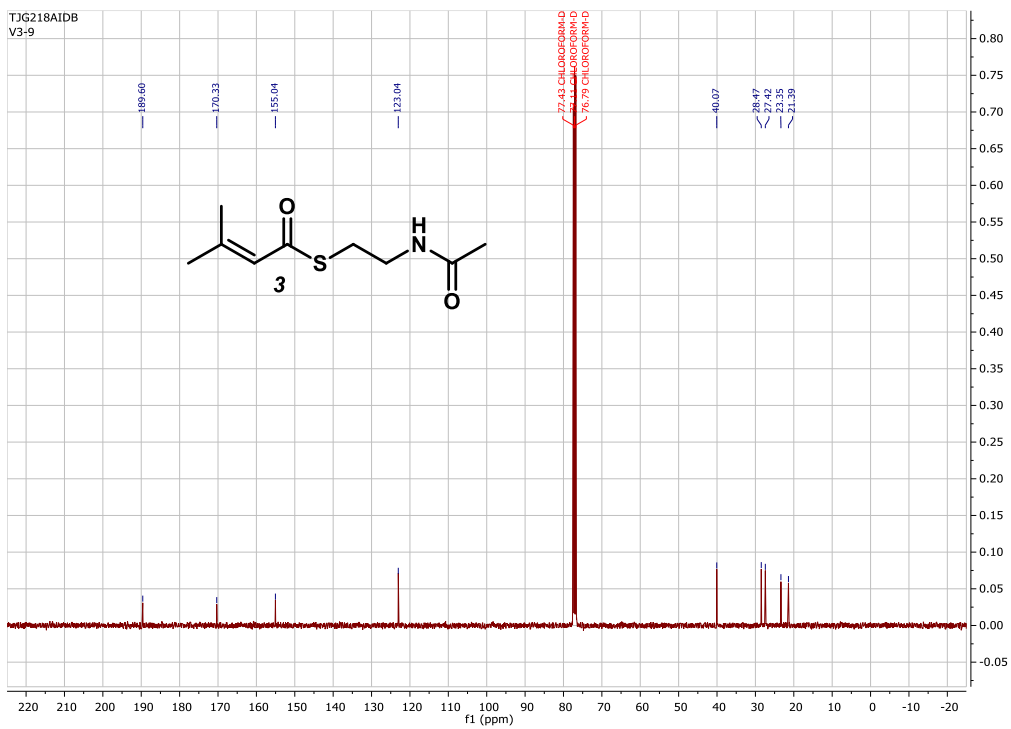
# <sup>1</sup>H NMR



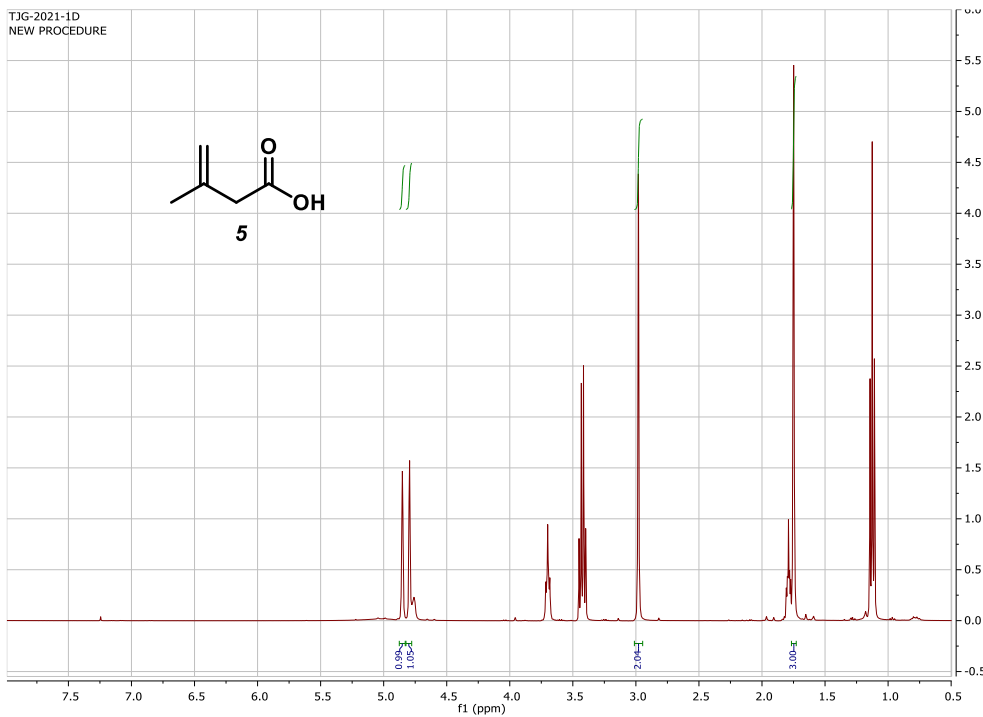
# <sup>1</sup>H NMR



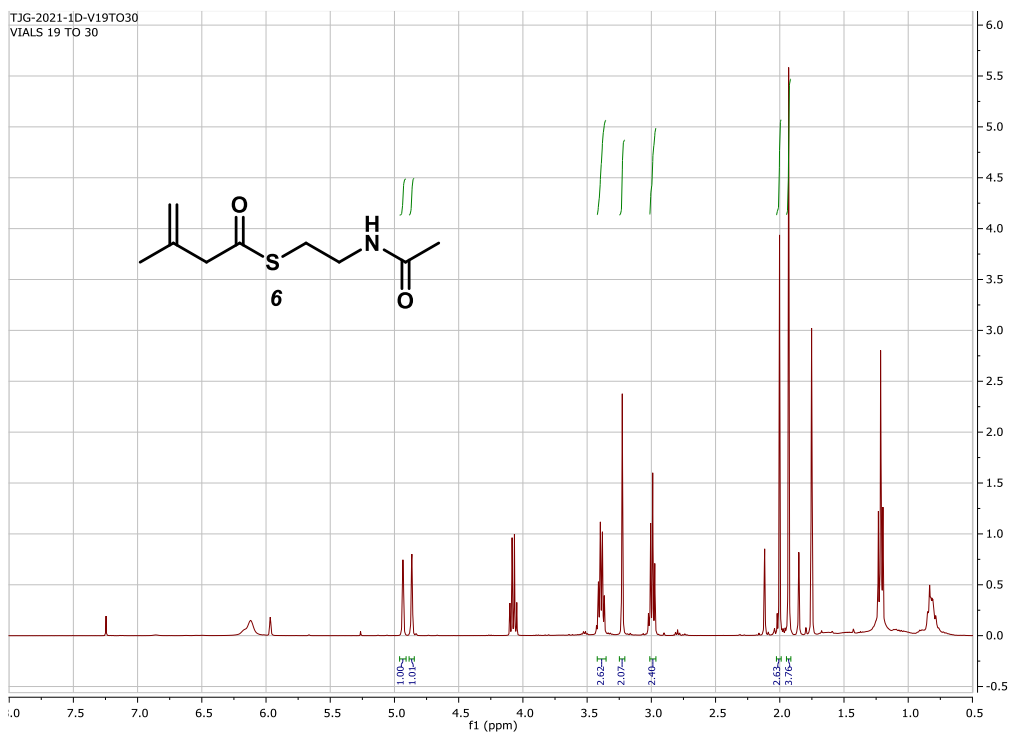
# <sup>13</sup>C NMR



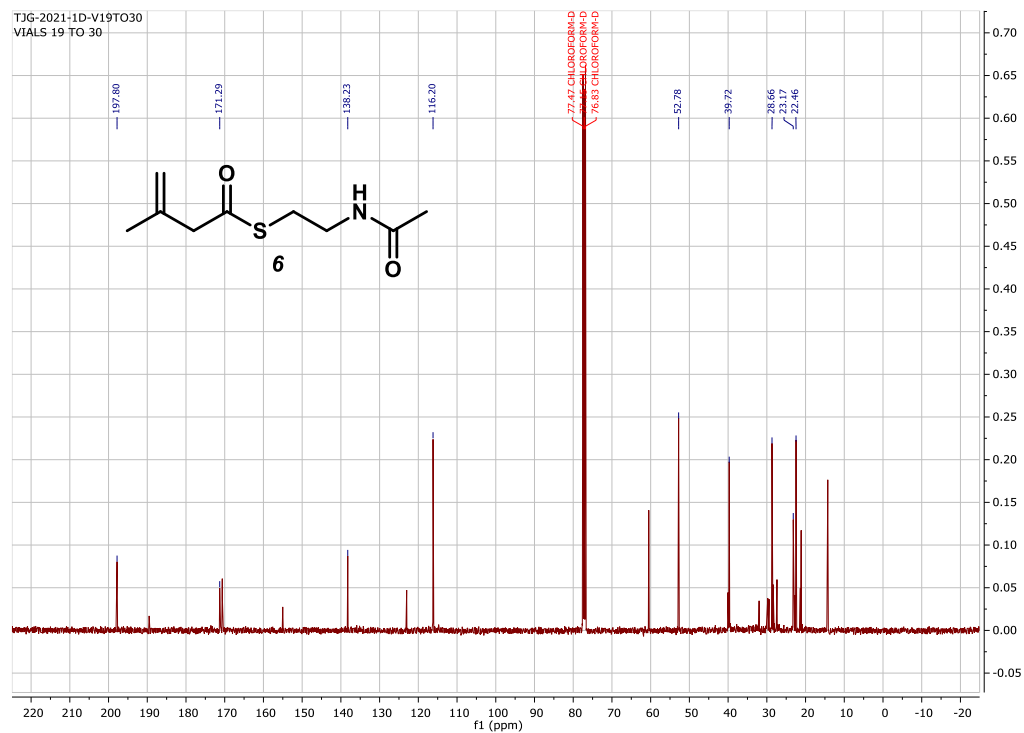
# <sup>1</sup>H NMR



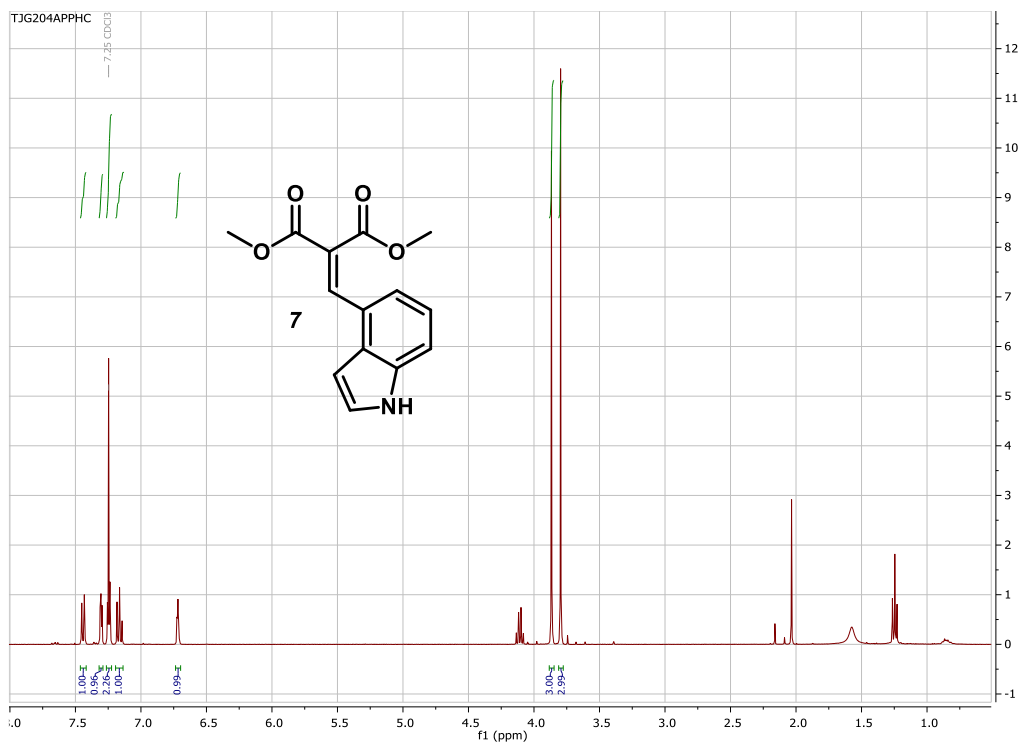
# <sup>1</sup>H NMR



# <sup>13</sup>C NMR



# <sup>1</sup>H NMR



# <sup>13</sup>C NMR

